Inter-laboratory comparison of δ^{13}C and δD measurements of atmospheric CH$_4$ for combined use of datasets from different laboratories

Taku Umezawa[1,2], Carl A. M. Brenninkmeijer[1], Thomas Röckmann[3], Carina van der Veen[3], Stanley C. Tyler[4,5], Ryo Fujita[6], Shinji Morimoto[6,7], Shuji Aoki[6], Todd Sowers[8], Jochen Schmitt[9], Michael Bock[9], Jonas Beck[9], Hubertus Fischer[9], Sylvia E. Michel[10], Bruce H. Vaughn[10], John B. Miller[10], James W. C. White[10], Gordon Brailsford[11], Hinrich Schaefer[11], Peter Sperlich[11], Willi A. Brand[12], Michael Rothe[12], Thomas Blunier[13], David Lowry[14], Rebecca E. Fisher[14], Euan G. Nisbet[14], Andrew L. Rice[15], Peter Bergamaschi[16], Cordelia Veidt[17] and Ingeborg Levin[17]

[1]Max Planck Institute for Chemistry, 55128 Mainz, Germany
[2]National Institute for Environmental Studies, Tsukuba 305-8506, Japan
[3]Institute for Marine and Atmospheric research Utrecht, Utrecht University, Utrecht, The Netherlands
[4]Earth System Science Department, University of California, Irvine, USA
[5]Chemistry Department, Norco College, Norco, CA 92860, USA
[6]Center for Atmospheric and Oceanic Studies, Graduate School of Science, Tohoku University, Sendai, Japan
[7]National Institute of Polar Research, Tokyo, Japan
[8]Pennsylvania State University, University Park, Pennsylvania 16802, USA
[9]Climate and Environmental Physics, Physics Institute and Oeschger Center for Climate Change Research, University of Bern, 3012 Bern, Switzerland
[10]Institute of Arctic and Alpine Research, University of Colorado Boulder, Boulder, Colorado, USA
[11]National Institute of Water and Atmospheric Research, Wellington 6021, New Zealand
[12]Max Planck Institute for Biogeochemistry, 07745 Jena, Germany
[13]Center for Ice and Climate, University of Copenhagen, Copenhagen, Denmark
[14]Department of Earth Sciences, Royal Holloway, University of London, Egham, UK
[15]Department of Physics, Portland State University, Portland, OR 97207, USA
[16]European Commission Joint Research Centre, Ispra (Va), Italy
[17]Institute for Environmental Physics, Heidelberg University, 69120 Heidelberg, Germany

Correspondence to: Taku Umezawa (umezawa.taku@nies.go.jp)

Abstract. We report results from a worldwide inter-laboratory comparison of samples among laboratories that measure (or measured in the past) stable carbon and hydrogen isotope ratios of atmospheric CH$_4$ (δ^{13}C-CH$_4$ and δD-CH$_4$). The offsets among the laboratories are larger than the

measurement reproducibility of individual laboratories. To disentangle plausible measurement offsets, we evaluated and critically assessed a large number of intercomparison results, some of which have been documented previously in the literature. The results indicate significant offsets of δ^{13}C-CH$_4$ and δD-CH$_4$ measurements among datasets reported from different laboratories; the differences among laboratories at modern atmospheric CH$_4$ level spread over ranges of 0.5 ‰ for δ^{13}C-CH$_4$ and 13 ‰ for δD-CH$_4$. The intercomparison results summarized in this study may be of help for future attempts to harmonize δ^{13}C-CH$_4$ and δD-CH$_4$ datasets from different laboratories in order to jointly incorporate them into modelling studies. However, establishing such a merged dataset, which includes δ^{13}C-CH$_4$ and δD-CH$_4$ data from multiple laboratories with desirable compatibility, is still challenging due to differences among laboratories in instrument settings, correction methods, traceability to reference materials and long-term data management. Further efforts are needed to identify causes of the inter-laboratory measurement offsets and to decrease those towards the best use of available δ^{13}C-CH$_4$ and δD-CH$_4$ datasets.

1 Introduction

Methane (CH$_4$) is an important anthropogenic and natural greenhouse gas, and it also has a large role in atmospheric chemistry through its reaction with the hydroxyl radical. Since individual CH$_4$ source types have characteristic isotope signatures and loss processes are associated with specific kinetic isotope effects, carbon and hydrogen isotope ratios of CH$_4$ (δ^{13}C-CH$_4$ and δD-CH$_4$) have been useful to constrain the global CH$_4$ budget. Dictated by global mass balance, the average isotopic composition of CH$_4$ in the atmosphere (δ^{13}C-CH$_4$ or δD-CH$_4$) equals the flux-weighted isotopic composition of the sources, corrected for the total kinetic isotope effects of removal processes (e.g. Stevens and Rust, 1982; Cicerone and Oremland, 1988; Quay et al., 1991, 1999; Miller et al., 2002; Turner et al., 2017; Rigby et al., 2017). It has been pointed out that assignment of representative isotopic signatures of various CH$_4$ sources remains uncertain due to their large spatial and temporal variability across the globe (e.g. Sherwood et al., 2017), which could result in large uncertainties of isotope-based estimates of the global CH$_4$ budget (Schwietzke et al., 2016). Nonetheless, the value of isotope measurements was amply demonstrated by recent studies which suggested shifts in the global CH$_4$ source over the last decades

(Schaefer et al., 2016; Rice et al., 2016; Nisbet et al., 2016; Schwietzke et al., 2016); without isotopic analyses such conclusions would have been difficult to achieve. The isotopic ratios are commonly reported using the delta notation:

$$\delta = \frac{R_{sample}}{R_{standard}} - 1 \qquad (1)$$

5   where R represents the atomic ratio of the less abundant over the most abundant isotope in the sample and the standard, respectively. Conventionally, measured values are reported relative to the international isotope scales VPDB for δ^{13}C-CH$_4$ and VSMOW for δD-CH$_4$ in per mil.

Given that the atmospheric lifetime of CH$_4$ is about a decade, its variation in background air is relatively small. For that reason, its mole fraction and isotopic measurements have to be made with high
10   precision and accuracy. For δ^{13}C-CH$_4$ and δD-CH$_4$, researchers have achieved measurement reproducibility of < 0.1 ‰ for δ^{13}C-CH$_4$ and < 2 ‰ for δD-CH$_4$. Incorporating δ^{13}C-CH$_4$ and δD-CH$_4$ datasets in chemistry transport models is useful to quantitatively separate different CH$_4$ source categories and such attempts have been contributed to reduction of uncertainties in the global CH$_4$ budget (e.g. Fung et al., 1991; Hein et al., 1997; Mikaloff Fletcher et al., 2004a, 2004b; Monteil et al.,
15   2011; Kirschke et al., 2013; Ghosh et al., 2015; Rice et al., 2016; Schaefer et al., 2016; Schwietzke et al., 2016; Röckmann et al., 2016; Turner et al., 2017; Rigby et al., 2017). However, although an increasing number of δ^{13}C-CH$_4$ and δD-CH$_4$ data has been reported over the last decades, significant measurement offsets among laboratories have been found for both δ^{13}C-CH$_4$ (e.g. Levin et al., 2012) and δD-CH$_4$ (Bock et al., 2014). It is clear that both traceability to the standard scales and inter-
20   laboratory comparisons (intercomparisons) are indispensable for combined use of δ^{13}C-CH$_4$ and δD-CH$_4$ data from different laboratories. Many such intercomparisons have already been made, either on an ad hoc basis or on a more organized scale. However, a systematic evaluation of the underlying calibrations and related measurement offsets among laboratories has been lacking. It is also noted that some measurement programs for δ^{13}C-CH$_4$ and/or δD-CH$_4$ have been discontinued, and maintaining
25   access to such datasets including well-established inter-laboratory offsets is important. Here we combine and evaluate the existing comparison results to quantify inter-laboratory measurement differences in order to facilitate the use of δ^{13}C-CH$_4$ and δD-CH$_4$ data. This study therefore opens the

possibility for merging historic CH_4 isotope data reported from multiple laboratories (i.e. synthesis analysis of the existing datasets) for better understanding of the global CH_4 budget.

We first present a technical overview of atmospheric $\delta^{13}C$-CH_4 and δD-CH_4 measurements and potential causes of measurement offsets among currently available datasets (section 2), and then we summarize

5 measurement methods by the laboratories that have conducted $\delta^{13}C$-CH_4 and δD-CH_4 measurements for air and ice core samples (section 3). In section 4, we report new intercomparison exercises between some groups. We then link the intercomparison results through survey of previous published intercomparisons and provide the current best estimates of measurement offsets among datasets from different laboratories (section 5). Finally, we summarize the current status and briefly discuss possible

10 causes of the measurement offsets as well as remaining issues that should be kept in mind for combined use of currently existing datasets of isotopic composition of CH_4 (section 6).

2 Overview of Atmospheric $\delta^{13}C$-CH_4 and δD-CH_4 Measurement Techniques

2.1 IRMS Measurements for $\delta^{13}C$-CH_4 and δD-CH_4

In the 1990s, atmospheric $\delta^{13}C$-CH_4 (δD-CH_4) was analyzed using an offline technique in which CH_4

15 was separated from sample air and converted to CO_2 (H_2) for subsequent offline $\delta^{13}C$-CH_4 (δD-CH_4) analyses by dual-inlet isotope ratio mass spectrometry (DI-IRMS) (e.g. Stevens and Rust, 1982; Lowe et al., 1991; Quay et al., 1991, 1999; Sugawara et al., 1996; Poß, 2003). The original methodology was based on the combustion of CH_4 in sample air, with interfering compounds such as CO_2, H_2O, N_2O, CO and non-methane hydrocarbons being removed cryogenically, chemically or by gas chromatography

20 before the CH_4 combustion. The number of measurements was limited not only because of laborious and time-consuming laboratory procedures but also because large volumes of air sample were required (> 100 L_{STP} for δD-CH_4). Later, a method based on continuous-flow gas chromatography isotope ratio mass spectrometry (GC-IRMS) technique combined with combustion and pyrolysis furnaces became available (Merritt et al. 1995; Burgoyne and Hayes, 1998; Hilkert et al., 1999), which dramatically

25 reduced time and efforts in the laboratory and likewise the amount of sample air required (now typically 100 mL_{STP}). Such systems are now used in most laboratories worldwide for acquiring $\delta^{13}C$-CH_4 and

δD-CH$_4$ data in the current and past atmosphere (Rice et al., 2001; Miller et al., 2002; Sowers et al., 2005; Ferretti et al., 2005; Morimoto et al., 2006; Fisher et al., 2006; Behrens et al., 2008; Umezawa et al., 2009; Brass and Röckmann, 2010; Sperlich et al., 2013; Schmitt et al., 2014; Bock et al., 2014; Brand et al., 2016; Röckmann et al., 2016). Although these systems use a similar measurement

5   principle, they vary in the use of pre-concentration of CH$_4$ in sample air, GC separation, and combustion/pyrolysis, data corrections and in the specific IRMS instrument among laboratories (see Schmitt et al., 2013, section 3 and Table 1). Besides analysis by mass spectrometry, laser-based spectroscopy has also been developed for atmospheric δ^{13}C-CH$_4$ and δD-CH$_4$ measurements (Bergamaschi et al., 2000; Eyer et al., 2016), but detailed discussion on the technique is beyond the

10   scope of this study.

2.2 Standard Scales

VPDB and VSMOW are the standard scales for δ^{13}C-CH$_4$ and δD-CH$_4$, respectively. To make measurements traceable to these standard scales, each laboratory needs to calibrate its laboratory reference gases against reference materials (RMs) with known values on the standard scales. In this

15   study, the term "calibration" means to measure a laboratory gas (for instance a laboratory working standard gas that is routinely compared with samples) against a standard at higher hierarchy level and to assign to that working standard a δ^{13}C-CH$_4$ or δD-CH$_4$ value traceable to the standard scale. In principle, all measurements at individual laboratories intend to ultimately anchor their working standards and sample gases to the VPDB or VSMOW scale using the RMs provided by the International

20   Atomic Energy Agency (IAEA) or National Institute of Standards and Technology (NIST) (Coplen et al., 2006; Brand et al., 2014). However, since RMs and recommended calibration methods for measurements of δ^{13}C-CH$_4$ and δD-CH$_4$ in air have not yet been provided (Sperlich et al., 2012, 2016), individual groups have developed their own calibration strategies.

Since δ^{13}C-CH$_4$ measurement by IRMS is made by δ^{13}C analysis in CO$_2$ oxidized from CH$_4$ in air, some

25   laboratories use pure CO$_2$ gases as a working standard. In many laboratories, these internal CO$_2$ standard gases were calibrated against pure CO$_2$ produced from the primary anchor of the VPDB scale NBS-19 or other RMs by using DI-IRMS (Table 1). Since the typical atmospheric δ^{13}C-CH$_4$ value

(about −47 ‰) differs considerably from the $\delta^{13}C$ value of NBS-19 (+1.95 ‰), some laboratories have used other RMs with VPDB values close to the atmospheric $\delta^{13}C\text{-}CH_4$ such as LSVEC, IAEA-CO-9 and RM 8563 as a second anchoring point of the VPDB scale (see Table 1) in order to minimize the risk for significant errors in realization of the standard scale (due to scale contraction or ^{17}O correction,

5 described in the following sections). A standard scale established this way at an individual laboratory was often propagated to laboratory-internal CO_2 standard gases at lower hierarchy levels, and they were used as the reference in DI-IRMS or GC-IRMS measurement of CO_2 processed from CH_4 in sample air. Ideally, this accurately links $\delta^{13}C\text{-}CH_4$ of the sample to the international isotope scale. In contrast, it has been recommended that a measured value of a sample is determined against a reference gas that

10 undergoes the all preparation steps in the sample measurement line in order to cancel out possible isotopic fractionations due to different treatment between the sample and reference gases (principle of identical treatment; Werner and Brand, 2001). This concept has been taken into account in some laboratories; a working standard is calibrated for $\delta^{13}C\text{-}CH_4$ and sample measurements are referenced by comparison with measurements of that working standard processed in the same manner (e.g. Brand et

15 al., 2016). Despite intensions for best traceability to RMs, the variety of calibrations has resulted in diverse realizations of the VPDB scale across $\delta^{13}C\text{-}CH_4$ measurement programs. As in Table 1, the different RMs that have been applied for $\delta^{13}C\text{-}CH_4$ calibration include NBS-19 (limestone), IAEA-CO-9 (barium carbonate), LSVEC (lithium carbonate), and RM 8562–8564 (CO_2); see Coplen et al. (2006), Brand et al. (2014) and Sperlich et al. (2016). It is also noted that uncertainty of assigned values for

20 these RMs ranges up to a few tenths ‰ and the assigned values have been revised over time (Brand et al., 2014), which might have complicated the realization of the standard scale at each laboratory. Furthermore, most of these RMs are in different chemical forms, and different isotopic fractionations may have occurred during acid digestion to CO_2, which could have biased calibrations at each laboratory. Lastly, WMO (2016) has reported exhaustion of NBS-19 and instability of LSVEC, both of

25 which are critical RMs for the VPDB scale. Associated possible revision of $\delta^{13}C$ values of RMs in the future will affect consistency of the datasets from different laboratories.

For $\delta D\text{-}CH_4$, in the conventional offline measurements, CH_4 in sample air needs to be processed to H_2O followed by reduction to H_2 for a subsequent DI-IRMS measurement. GC-IRMS requires pyrolysis of

CH$_4$ to H$_2$. Therefore, individual laboratories have prepared internal standards of H$_2$O (liquid) or H$_2$ (gas), which were calibrated against primary RMs (water) or H$_2$ reference gases certified for δD (Table 1). Although the situation is less complicated compared to δ^{13}C-CH$_4$ in terms of variety in chemical properties of RMs, the lack of RMs for δD-CH$_4$ forced laboratories to develop their calibration method

5   standard scale individually. It is also noted that, similar to δ^{13}C-CH$_4$, principle of identical treatment has not been followed strictly at the all laboratories. If not followed, sample measurements are subject to subtle changes in conditions of the all preparation steps (e.g. conversion of CH$_4$), while such changes do not affect the measured value of a reference gas injected directly to the IRMS.

2.3 Scale Contraction

10   It has been found that cross contamination between sample and reference CO$_2$ gases shrinks the δ^{13}C distance measured on DI-IRMS (Meijer et al., 2000; Verkouteren et al., 2003a, 2003b). This effect is known as scale contraction or η effect, and the magnitude is specific to the IRMS instrument and its settings. Since the VPDB scale for δ^{13}C-CH$_4$ has been realized and propagated via CO$_2$ calibrations by DI-IRMS at individual laboratories, the instrument-dependent scale contraction effect could have

15   caused a significant difference in measurement values, especially at the low δ^{13}C values of atmospheric CH$_4$ of about −47 ‰ (Wendeberg et al., 2013).

2.4 [17]O Correction

For measurement of δ^{13}C-CH$_4$ by IRMS, CH$_4$ is first oxidized to CO$_2$ and the different isotopic variants of the produced CO$_2$ are then registered on Faraday cups with mass to charge ratios *m/z* of 44, 45 and

20   46. Since the raw ion beam intensity for *m/z* = 45 is the sum of ^{13}C^{16}O$_2$ and ^{12}C^{17}O^{16}O, the final δ^{13}C value is obtained by correcting for the contribution of the ^{17}O containing isotopologue, known as ^{17}O correction (e.g. Assonov and Brenninkmeijer, 2003). Several algorithms such as Craig (1957) and Santrock et al. (1985) have been suggested (see Assonov and Brenninkmeijer (2003) and references therein) and implemented into software/programs of the IRMS companies and individual laboratories.

25   Assonov and Brenninkmeier (2003) showed that the bias caused by different ^{17}O-correction algorithms

could exceed general repeatability achieved by IRMS measurements. The ^{17}O correction method of each laboratory is listed in Table 1.

2.5 Krypton Interference in GC-IRMS

The transition from DI-IRMS to GC-IRMS analyses reduced the analytical effort, but also introduced complications that were initially not recognized and taken into account. It was recently found that atmospheric krypton (Kr) interferes with the $\delta^{13}C$-CH_4 GC-IRMS analysis if Kr is present in the ion source during the data acquisition of the CO_2 peak generated from CH_4 oxidation (hereafter CH_4-derived CO_2 peak) (Schmitt et al., 2013). Thus the $\delta^{13}C$-CH_4 measurements on a GC-IRMS system can be biased if Kr is not separated sufficiently from either CH_4 or from the CH_4-derived CO_2 peak after the CH_4 combustion. Schmitt et al. (2013) demonstrated that the doubly charged krypton isotope $^{86}Kr^{2+}$, produced in the ion source of an IRMS, can cause lateral tailing extending into the Faraday cups used for $\delta^{13}C$ analysis (i.e. m/z of 44, 45 and 46), which compromises the measured signal of the CH_4-derived CO_2 peak. This effect had not been recognized for more than a decade since the early years of GC-IRMS measurements (Merritt et al., 1995), and thus has not been taken into account in many datasets of atmospheric $\delta^{13}C$-CH_4 reported in the meantime (e.g. Miller et al., 2002; Morimoto et al., 2006; Fisher et al., 2011; Röckmann et al., 2011; Umezawa et al., 2012a, 2012b). Furthermore, because the Kr effect is system-dependent and variable with time (Schmitt et al., 2013), applying plausible corrections to past data may not be feasible. Likewise, several gas species including Kr can affect δD-CH_4 measurements, and this effect is also system-dependent (Bock et al., 2014).

Several solutions have been suggested to eliminate or account for the Kr interference (Schmitt et al., 2013). Among them, three methods have been implemented at different laboratories (Table 1). Briefly, (1) After the CH_4 oxidation to CO_2, Kr is separated from the CH_4-derived CO_2 by using a post combustion separation column (PCS) or cryogenically. (2) An offset due to the Kr interference is estimated by comparison with a DI-IRMS measurement (DI-offset). (3) The Kr interference peak is subtracted from the raw ion current time series of the IRMS acquisition (raw ion current correction). More detailed description has been presented in Schmitt et al. (2013).

3. Measurements of Participating Laboratories

In this section, we briefly document measurement systems of individual laboratories for ease of reference in the following intercomparisons (sections 4 and 5). For details, we refer to more dedicated publications listed in Table 1. The table also visualizes differences among laboratories in terms of possible causes of the measurement offsets described in section 2.

3.1 NIWA

National Institute for Water and Atmospheric Research (NIWA, originally INS (Institute of Nuclear Sciences), later INGS (Institute of Nuclear and Geological Sciences) until 1992) successfully initiated systematic measurements of atmospheric δ^{13}C-CH$_4$ by means of offline CH$_4$ separation and conversion followed by a DI-IRMS measurement in 1988 (Lowe et al., 1988, 1991). A suite of CO$_2$ working gases with δ^{13}C-CH$_4$ values around −47 ‰ referenced to IAEA materials were utilized to calibrate the measurements. An overall reproducibility of the δ^{13}C-CH$_4$ measurement was evaluated to be 0.02 ‰ (Lowe et al., 1991). The δ^{13}C-CH$_4$ measurements at NIWA are ultimately calibrated against CO$_2$ produced from NBS-19, IAEA-CO-9 and LSVEC. The long-term δ^{13}C-CH$_4$ records have been presented since then (Lowe et al., 1994, 1997, 2004; Bergamaschi et al., 2001; Schaefer et al., 2016). Bromley et al. (2012) reported that repeated measurements of the two working reference gases and archived air indicated no detectable drift over 16 years since 1992. NIWA also operates a GC-IRMS system since 2004 (Ferretti et al., 2005) with reproducibility of 0.1 ‰. The Kr interference on the GC-IRMS δ^{13}C-CH$_4$ measurement has been identified, which is corrected by an offset relative to the conventional DI-IRMS measurement (see section 4.1).

3.2 IMAU

The GC-IRMS system at the Institute for Marine and Atmospheric research Utrecht (IMAU) has been described by Brass and Röckmann (2010). The measurement reproducibility is estimated to be 0.07 ‰ and 2.3 ‰ for δ^{13}C-CH$_4$ and δD-CH$_4$, respectively. Sample air is measured against reference air that is processed in the GC-IRMS system in the same manner as a sample. The IMAU δ^{13}C-CH$_4$ standard scale is based on a set of assigned values for 13 firn air samples measured at Max Planck Institute for

Chemistry (MPIC) (Bräunlich et al., 2001) and they are ultimately referenced to a CO_2 gas produced from NBS-19 (Röckmann, 1998; Bergamaschi et al., 2000). The δD-CH_4 standard scale is based on a set of reference gases originally produced at MPIC (see section 2.3). These calibration details have been documented also by Sperlich et al. (2016). The IMAU system was originally affected by Kr but later

5   modified to remove this interference. A correction was applied for data obtained before the system modification (Schmitt et al., 2013).

3.3 MPIC

MPIC has reported $\delta^{13}C$-CH_4 and δD-CH_4 measurements at a baseline station (Bergamaschi et al., 2000) and for firn air samples (Bräunlich et al., 2001) based on an offline DI-IRMS measurement for

10   $\delta^{13}C$-CH_4 (Bergamaschi et al., 2000) and a tunable diode laser based absorption spectrometer (TDLAS) for δD-CH_4 (Bergamaschi et al., 1994). Some firn air measurements by Bräunlich et al. (2001) were performed by using a GC-IRMS system at Laboratory of Glaciology and Geophysics of the Environment. As described in section 3.2, the $\delta^{13}C$-CH_4 and δD-CH_4 standard scales of MPIC are basis of that of IMAU. For the $\delta^{13}C$-CH_4 DI-IRMS measurement, the CH_4-derived CO_2 was measured against

15   a working standard (pure CO_2) that was calibrated against NBS-19 on a DI-IRMS system (Röckmann, 1998; Bergamaschi et al., 2000). The MPIC δD-CH_4 scale is based on measurements of standard gases at the Bundesanstalt für Geowissenschaften und Rohstoffe, Hannover, Germany; CH_4 was combusted to CO_2 and H_2O, followed by reduction of H_2O to H_2 for subsequent DI-IRMS analysis on H_2; the calibration was made against VSMOW and SLAP (Bergamaschi et al., 2000). The measurements of

20   atmospheric $\delta^{13}C$-CH_4 and δD-CH_4 at MPIC were discontinued.

3.4 MPI-BGC

Max Planck Institute for Biogeochemistry (MPI-BGC) set up a GC-IRMS system for $\delta^{13}C$-CH_4 and δD-CH_4 measurements, and it has been operated for air samples collected at baseline stations (Brand et al., 2016). The long-term (3 years) reproducibility was assessed to be 0.12 ‰ for $\delta^{13}C$-CH_4 and 1.0 ‰ for

25   δD-CH_4. Initially, the GC-IRMS measurements had been anchored to a working standard air calibrated by IMAU. The Kr effect was eliminated by a PCS column, and the initial calibration has in the

meantime been replaced by a new primary calibration, where measurements are ultimately anchored to NBS-19 and LSVEC for δ^{13}C-CH$_4$ and VSMOW-2 and SLAP-2 for δD-CH$_4$ (Sperlich et al., 2016). This calibration, termed JRAS-M16, is the basis for the δ^{13}C-CH$_4$ and δD-CH$_4$ values from MPI-BGC reported in this manuscript.

3.5 UCI

University of California Irvine (UCI) measured atmospheric δ^{13}C-CH$_4$ by offline DI-IRMS and δD-CH$_4$ by GC-IRMS (Tyler et al., 1999, 2007; Kai et al., 2011). The UCI GC-IRMS system for both δ^{13}C-CH$_4$ and δD-CH$_4$ has been described in detail by Rice et al. (2001). The measurement reproducibility of the GC-IRMS system was estimated to be 0.05 ‰ and 1.5 ‰ for δ^{13}C-CH$_4$ and δD-CH$_4$, respectively, while that of the offline DI-IRMS δ^{13}C-CH$_4$ measurement was 0.05 ‰. Samples were measured against laboratory working standard gases of pure CO_2 for δ^{13}C-CH$_4$ and pure H_2 for δD-CH$_4$. The δ^{13}C-CH$_4$ calibration is based on a CO_2 reference gas provided by NIWA, which was compared with CO_2 produced from NBS-19 and IAEA-CO-9 (Lowe et al., 1999). The δD-CH$_4$ calibration is referenced to three H_2 gas cylinders purchased from Oztech Gas Company (Rice et al., 2001). The possible Kr interference on the GC-IRMS system is unclear (the laboratory is now closed), but it appears that the Kr effect had been avoided using liquid nitrogen cooling of the GC column as surmised by Schmitt et al. (2013).

3.6 TU

The GC-IRMS system at Tohoku University (TU) has been described by Umezawa et al. (2009). The measurement reproducibility is estimated to be 0.08 ‰ for δ^{13}C-CH$_4$ and 2.2 ‰ for δD-CH$_4$. Sample measurements are made against pure CO_2 and H_2 working standard gases for δ^{13}C-CH$_4$ and δD-CH$_4$, respectively. The δ^{13}C-CH$_4$ calibration is based on a CO_2 primary gas produced from NBS-19. The H_2 working standard for δD-CH$_4$ measurement is referenced to water laboratory standards that are calibrated against VSMOW and SLAP. Measured δD-CH$_4$ values are corrected so that the value of a laboratory test gas is kept constant over time to take into account fluctuations in the measured value due to the condition of the pyrolysis furnace (Umezawa et al., 2009, 2012a). The Kr interference on the

δ^{13}C-CH$_4$ measurement was identified, but modification or correction has not been implemented. It has been documented that δ^{13}C-CH$_4$ measurement at TU shifted by +0.27 ‰ after July 2008 (the cause of this sudden shift has yet to be identified) and measurements afterwards were corrected for this value to keep the data consistency (Umezawa et al., 2012a, 2012b). Note that TU made rigorous re-evaluation of the long-term measurements of their working standard gas recently, and the TU δ^{13}C-CH$_4$ datasets will be revised accordingly. Therefore, the comparison numbers presented here are not comparable to those for earlier publications (Umezawa et al., 2009, 2011, 2012a, 2012b).

3.7 NIPR

National Institute of Polar Research (NIPR) reported δ^{13}C-CH$_4$ measurements at an Arctic site using a GC-IRMS system (Morimoto et al., 2006). The measurement reproducibility was evaluated to be 0.06 ‰. The δ^{13}C-CH$_4$ calibration follows same procedure as TU. By injecting different quantities of Kr, it was confirmed that ambient Kr does not significantly interfere with the δ^{13}C-CH$_4$ measurements at NIPR.

3.8 UW

University of Washington (UW) reported extensive δ^{13}C-CH$_4$ and δD-CH$_4$ measurements using an offline DI-IRMS system (Quay et al., 1991, 1999). The reproducibility was estimated to be 0.1 ‰ for δ^{13}C-CH$_4$ and 3–4 ‰ for δD-CH$_4$. The δ^{13}C-CH$_4$ calibration is based on measurements against NBS-19 (Quay et al., 1999), while the earlier measurements were calibrated against NBS-20 and NBS-16 (Quay et al., 1991). The δD-CH$_4$ was anchored to calibration by VSMOW and SLAP. Systematic measurements of air standards showed that no significant time shift (+0.001±0.002 ‰ yr^{-1}) affected their δ^{13}C-CH$_4$ dataset for 1988–1995 (Quay et al., 1999).

3.9 UHEI

University of Heidelberg (UHEI) carried out δ^{13}C-CH$_4$ measurements by DI-IRMS (Levin et al., 1999, 2012). The typical measurement reproducibility was evaluated to be 0.05 ‰ (Levin et al., 1999). The UHEI δ^{13}C-CH$_4$ measurements are calibrated against CO$_2$ reference materials (RM 8562, RM 8563 and RM 8564) (Behrens et al., 2008). Although reported previously only for signatures of source CH$_4$

(Levin et al., 1993), UHEI also made offline δD-CH$_4$ measurements on atmospheric samples by DI-IRMS and TDLAS (Poß, 2003). The δD-CH$_4$ measurements by DI-IRMS were made on pure H$_2$ (H$_2$O from CH$_4$ oxidation converted to H$_2$ with zinc as catalyst) and were calibrated against VSMOW and SLAP. Note that UHEI recently re-evaluated all their atmospheric δ^{13}C-CH$_4$ and δD-CH$_4$ measurements

5   rigorously, based on the history of laboratory standards used; therefore, comparison numbers published in earlier works are not comparable to the revised values presented here.

3.10 INSTAAR

Institute of Arctic and Alpine Research (INSTAAR) of the University of Colorado Boulder has measured δ^{13}C-CH$_4$ and, intermittently, δD-CH$_4$ using a GC-IRMS system for flask air samples from

10 the cooperative sampling network of National Oceanic and Atmospheric Administration (NOAA) (Miller et al., 2002). Reproducibilities of the δ^{13}C-CH$_4$ and δD-CH$_4$ measurements are evaluated to be 0.08 ‰ and 2 ‰, respectively (Miller et al., 2002; White et al., 2016). The INSTAAR δ^{13}C-CH$_4$ measurement currently follows the UCI calibration, while the δD-CH$_4$ measurement is not explicitly anchored to the VSMOW scale (White et al., 2016). The Kr interference on the δ^{13}C-CH$_4$ measurement

15 is significant, and a PCS column was therefore implemented into the system in May 2017. Correction of the data for the Kr interference (1998–present) is under evaluation. Of the data presented here, only the ice core intercomparison round robin (section 3.4) and the INSTAAR-MPI-BGC comparison (section 3.5) have not been interfered by Kr.

3.11 RHUL

20 Royal Holloway University of London (RHUL) measured atmospheric δ^{13}C-CH$_4$ using an offline DI-IRMS technique (Lowry et al., 2001) and a GC-IRMS system (Fisher et al., 2006, 2011; Nisbet et al., 2016). Reproducibility of the DI-IRMS measurement was evaluated to be 0.04 ‰ (Lowry et al., 2001) and that by the GC-IRMS is 0.05 ‰ (Fisher et al., 2006). They made δ^{13}C-CH$_4$ calibrations ultimately to IAEA carbonate materials NBS-19 and IAEA-CO-9 (Lowry et al., 2001; Fisher et al., 2006). Note

25 that RHUL applies an offset correction of −0.20 ‰ for the measured value by GC-IRMS (sections 4.6 and 5.11).

3.12 PDX

Portland State University (PDX) reported δ^{13}C-CH$_4$ and δD-CH$_4$ measurements for archive air samples (Rice et al., 2016). The PDX measurement system has been described in Teama (2013) with some updates since Rice et al. (2001). The δ^{13}C-CH$_4$ and δD-CH$_4$ reproducibilities are 0.07 ‰ and 2.0 ‰, respectively, and PDX shares the standard scales with UCI for both δ^{13}C-CH$_4$ and δD-CH$_4$ (Rice et al., 2016).

3.13 PSU

Pennsylvania State University (PSU) reported δ^{13}C-CH$_4$ and δD-CH$_4$ data from ice cores and firn air using a GC-IRMS system (e.g. Sowers et al., 2005; Sowers, 2010). The overall measurement reproducibility including every step for ice core measurements was evaluated to be 0.3 ‰ for δ^{13}C-CH$_4$ and 3 ‰ for δD-CH$_4$ (Sowers, 2010). The PSU δ^{13}C-CH$_4$ measurements are calibrated against CO$_2$ RMs (RM 8563 and RM 8564). The δD-CH$_4$ calibration is made against H$_2$ gas bottles from Oztech Gas Company (Sowers, 2006).

3.14 UB

University of Bern (UB) makes δ^{13}C-CH$_4$ measurements from ice cores using a GC-IRMS system with an overall reproducibility of 0.15 ‰ (Schmitt et al., 2014; Bock et al., 2017). The UB measurements are referenced to a whole-air working standard with CH$_4$ mole fraction of 1508.2 ppb and an assigned δ^{13}C-CH$_4$ value of −47.34±0.02 ‰ (named "Boulder, CA08289" in Schmitt et al., 2014). This value is anchored to the standard scale used at INSTAAR (section 3.10). UB also measures δD-CH$_4$ for ice core samples (Bock et al., 2010, 2014, 2017). The overall measurement precision for ice core sample (including extraction of air from an ice sample) was evaluated to be 2.3 ‰. The UB δD-CH$_4$ measurement is referenced by using an ambient air cylinder (named "Air Controlé") with a δD-CH$_4$ value of −93.6±2.8 ‰, which was cross-referenced to a high pressure cylinder filled at the Alert Station ("Alert 2002/11" with δD-CH$_4$ of −82.2±1.0 ‰) analyzed on the scale maintained at UHEI (Bock et al., 2010, 2014). However, this value has to be corrected to −85.2±1.0 ‰ to account for the recent re-evaluation at UHEI (section 3.9). All UB data published after 2011 are free of Kr interference.

3.15 AWI

Alfred Wegener Institute Helmholtz Centre for Polar and Marine Research (AWI) reported δ^{13}C-CH$_4$ measurements from ice cores using a GC-IRMS system (Behrens et al., 2008; Fischer et al., 2008; Möller et al., 2013). The measurement reproducibility was estimated to be 0.2 ‰. The δ^{13}C-CH$_4$ measurements employed the UHEI standard scale via comparison of measurements of an air sample collected at Neumayer Station, Antarctica (Möller et al., 2013).

3.16 CIC

Centre for Ice and Climate (CIC) of the Niels Bohr Institute has reported δ^{13}C-CH$_4$ measurements from ice cores (Sperlich et al., 2015) using a GC-IRMS system with measurement reproducibility of 0.09 ‰ (Sperlich et al., 2013). CIC also set up an offline combustion system for samples with large amount of CH$_4$, which is combined with DI-IRMS for δ^{13}C-CH$_4$ and with either a high Temperature Conversion/Elemental Analyser (TC/EA) coupled to IRMS or laser spectroscopy for δD-CH$_4$ (Sperlich et al., 2012); the measurement reproducibility is 0.04 ‰ for δ^{13}C-CH$_4$ and 0.7 ‰ for δD-CH$_4$. The CIC measurements are referenced to RM 8563 for δ^{13}C-CH$_4$ and VSMOW-2 and SLAP-2 for δD-CH$_4$. The combined uncertainty of this analytical system including the uncertainty of the entire traceability chain was estimated as 0.07 ‰ for δ^{13}C-CH$_4$ and 0.7 ‰ for δD-CH$_4$ (Sperlich et al., 2016).

4 Intercomparison Exercises

4.1 Intercomparison between UCI and IMAU

An intercomparison between UCI and IMAU was made by analyzing 6 air samples at both laboratories; the air samples were collected along a flight track of commercial aircraft in the upper troposphere in the early phase of the CARIBIC (Civil Aircraft for the Regular Investigation of the atmosphere Based on an Instrument Container) project (Brenninkmeijer et al., 1999). The original samples were collected into large stainless steel cylinders (21 L) and aliquots of them were transferred into smaller stainless steel canisters (~2.3 L) for storage after delivery to the MPIC laboratory. Different sub samples from identical original samples were sent to UCI and IMAU for analyses, and they were measured at UCI in

2008 and at IMAU in 2012 to 2013. The measurement results at both laboratories are summarized in Table 2. The result indicated significant differences of +0.42±0.04‰ for δ^{13}C-CH$_4$ (UCI value is higher than IMAU) and of −10.7±0.7‰ for δD-CH$_4$ (UCI value is lower than IMAU).

4.2 Intercomparison between TU/NIPR and IMAU

5 An intercomparison between TU/NIPR and IMAU was carried out during 2013–2015. The TU laboratory prepared four stainless steel canisters (~1 L) filled with dried ambient air (canisters MD1 and MD2) and CH$_4$-in-synthetic air gas (canisters MD3 and MD4) with CH$_4$ mole fractions ranging from 899 to 2117 ppb on the TU CH$_4$ scale (Aoki et al., 1992; Umezawa et al., 2014) (Table 3). The canisters were analyzed at TU and then sent to IMAU, after which they were sent back to TU and reanalyzed to

10 confirm the stability of the air samples in the canisters during the intercomparison exercise. The measurements at TU before and after the transport to IMAU throughout April 2013 to July 2015 indicated that possible drifts during canister storage and transportation are small (< 0.1 ‰ for δ^{13}C-CH$_4$ and < 3.5 ‰ for δD-CH$_4$). NIPR also measured the canisters for δ^{13}C-CH$_4$. The results indicate significant differences of +0.50±0.07 ‰ for δ^{13}C-CH$_4$ (TU value is higher than IMAU) and of

15 −13.9±0.9 ‰ for δD-CH$_4$ (TU value is lower than IMAU) (Table 3). The measurements of the four canisters at NIPR were +0.48±0.11 ‰ higher than IMAU. However, the differences of δ^{13}C-CH$_4$ measurements are smaller for the ambient air samples (MD1 and MD2) than the CH$_4$-in-synthetic air samples (MD3 and MD4). It is also noted that the δ^{13}C-CH$_4$ difference between the laboratories is largest for the low CH$_4$ mole fraction (~900 ppb) sample (MD3). The cause is unclear, but might be

20 related to (1) deviation in δ^{13}C-CH$_4$ of the latter samples from the typical atmospheric value, i.e., scale contraction effect, (2) difference in air matrix, i.e., natural versus synthetic air and (3) difference in linearity with respect to CH$_4$ mole fraction. This result therefore indicates that the measurement offset is not constant for a wide range of δ^{13}C-CH$_4$ values and CH$_4$ mole fractions as well as differences in air matrix. Since we focus in this study on comparison for atmospheric samples, the intercomparison

25 results for the ambient air samples are considered as inter-laboratory measurement offsets. The average differences for ambient air are +0.40±0.04 ‰ for TU and +0.31±0.03 ‰ for NIPR relative to IMAU. Likewise, the δD-CH$_4$ offset of TU versus IMAU is considered to be −13.1±0.6 ‰.

4.3 Intercomparison between UHEI and MPI-BGC

An intercomparison between UHEI and MPI-BGC was conducted in 2013 on six archived air samples from Neumayer station, Antarctica. These samples, collected in the time period from 1988 to 2008 had been analyzed by UHEI for δ^{13}C-CH$_4$ and δD-CH$_4$ by DI-IRMS (two samples were analyzed for δD-CH$_4$ additionally by TDLAS) during 2003–2010 and were stored in high-pressure cylinders. In 2013, duplicate aliquots were sampled in 1-L glass flasks and analyzed at MPI-BGC. The measurement results at both laboratories are summarized in Table 4. The results show insignificant measurement offsets of +0.02±0.05 ‰ for δ^{13}C-CH$_4$ and of +0.4±0.6 ‰ for δD-CH$_4$ (with the MPI-BGC values being more negative than those from UHEI in both cases).

4.4 Round Robin Comparison among Ice Core Analysis Laboratories

A round robin cylinder exercise was initiated to facilitate intercomparison of those laboratories who measure δ^{13}C-CH$_4$ and δD-CH$_4$ in ice core and firn air samples. Part of this exercise has been presented previously (Table 2 in Schmitt et al., 2013). Three high-pressure Al cylinders were filled with varying trace gas composition to mimic present day, pre-industrial and last-glacial air mole fractions. The CH$_4$ mole fractions of these cylinders were 1830.6 ppb (CA 03560), 904.0 ppb (CC 71560) and 372.2 ppb (CA 01179) on the NOAA-2004 CH$_4$ scale (Dlugokencky et al., 2005), respectively. The cylinders were shipped to the laboratories listed in Table 5 for analyses of all constituents that each lab was capable of measuring at that time. In Table 5, we list the δ^{13}C-CH$_4$ and δD-CH$_4$ results from each laboratory. The Kr interfering artefact associated with GC-IRMS δ^{13}C-CH$_4$ analyses was taken into account in many of the analyses (Schmitt et al., 2013). In some cases, aliquots from the tanks were measured using offline combustion to CO$_2$ followed by δ^{13}C-CH$_4$ analyses via conventional DI-IRMS. The cylinders were remeasured at PSU at the end of the round robin to verify that the isotopic composition had not shifted over the 9 years during the transportation of the cylinders. The difference between the 2007 and 2016 δ^{13}C-CH$_4$ measured at PSU were less than 0.14 ‰ for two of the three cylinders, indicating that the isotopic composition of the cylinder air was stable throughout the intercomparison exercise. The third cylinder (CA 01179) was 0.58 ‰ off from the original measurement, which is just outside the analytical uncertainty associated with PSU measurements. There may have been slight drift over the 9 years

between measurements, although the cause has yet to be resolved. The results of the δ^{13}C-CH$_4$ intercomparison showed agreement with the average standard deviation amongst all six participating laboratories better than 0.37 ‰ for the cylinders with high (CA 03560) and middle (CC 71560) mole fractions. δD-CH$_4$ results show more scatter due to the difficult nature of the measurements and the offset among the standard scales.

4.5 Intercomparison between INSTAAR and MPI-BGC

An intercomparison between INSTAAR and MPI-BGC was recently made by analyzing three air cylinders at both laboratories. They were measured at MPI-BGC between April and July of 2016 and at INSTAAR between May and June of 2017. Two of the cylinders have ambient CH$_4$ mole fraction (~1900 ppb; HUEY-001 and DEWY-001) and the other has a lower value (~1500 ppb; LOUI-001) (Table 6). In addition, air from another suite of cylinders was sampled into flasks at INSTAAR and sent to MPI-BGC. Measurements at MPI-BGC and INSTAAR were made in January–February of 2017 and May–June of 2017, respectively. The four cylinders (CART-001, STAN-001, KENN-001 and KYLE-001) have different CH$_4$ mole fractions and δ^{13}C-CH$_4$ values. The measurement results are summarized in Table 6. The INSTAAR data presented here were not interfered by Kr by installing a PCS column into the system. The results show significant but consistent measurement offsets of +0.28±0.01 ‰ for the five cylinders with different CH$_4$ mole fractions and ambient δ^{13}C-CH$_4$ values (with the INSTAAR values being more positive than those from MPI-BGC). The measurements for the cylinder with low δ^{13}C-CH$_4$ value were 0.60 ‰ off between both laboratories presumably due to the scale contraction effect. It is noted that the INSTAAR measurements without the Kr removal had yielded a higher δ^{13}C-CH$_4$ value (+0.44±0.02 ‰ relative to the MPI-BGC measurement) for one cylinder (LOUI-001), which presumably reflects the Kr interference pronounced at lower CH$_4$ mole fraction.

4.6 Intercomparison based on co-located samples through the NOAA cooperative sampling network

The Cooperative Flask Sampling Network, operated by the NOAA Global Monitoring Division, collects air samples from numerous sites around the world, and INSTAAR has analyzed those air samples for δ^{13}C-CH$_4$ since 1998. There are several sites where air sample collections by other laboratories have

been made concurrently. RHUL has analyzed air samples at Alert (ALT), Canada and Ascension Island (ASC), and NIWA has done at Baring Head (BHD), New Zealand. Although the individual laboratories do not measure the same sample air in these cases, these co-located air samples provide an opportunity for assessment of possible measurement offsets as examined previously (Levin et al., 2012). (1) For the

5 RHUL-INSTAAR difference, the δ^{13}C-CH$_4$ data at ALT during 2009–2014 and at ASC during 2010–2015 were compared to each other if both air samples were collected within a 10 hour interval. The ALT and ASC comparisons indicated that the INSTAAR measurement is +0.05±0.16 ‰ (N=350) and 0.00±0.17 ‰ (N=80) higher than RHUL, respectively. Note that, for this comparison, the RHUL GC-IRMS data were corrected by −0.20 ‰; the offset value was estimated from measurements of flasks

10 filled from two different cylinders (CH$_4$ in air, both at ambient mole fraction level, one at ambient δ^{13}C-CH$_4$ and the other at about −56 ‰ by spiking ^{13}C-depleted CH$_4$). (2) For the NIWA-INSTAAR comparison, the δ^{13}C-CH$_4$ data at BHD during 2009–2014 from both laboratories were compared if both air samples were collected within a 15 hour interval. The result indicates that the INSTAAR measurement is +0.08±0.11 ‰ (N=45) higher than NIWA.

15 **5 Measurement offsets among laboratories**

Here we revisit intercomparisons published previously. Some laboratories employed a standard scale from another laboratory. Such intercomparisons and inter-laboratory scale propagations reported in the literature are displayed in Fig. 1. In this section we review the previous and present intercomparison measurements and accordingly suggest plausible measurement offsets among different laboratories (Fig.

20 2). Relevant information is summarized in Table 1 and the subsections below correspond to those in section 3. Since some laboratories focus on δ^{13}C-CH$_4$ and δD-CH$_4$ measurements from ice core and firn air samples to elucidate changes of atmospheric CH$_4$ in the past, Fig. 2 also combines δ^{13}C-CH$_4$ and δD-CH$_4$ data both for the modern and past atmosphere. It is however noted that Fig. 2 suggests the measurement offsets at the modern CH$_4$ mole fraction and isotopic ratios and that such values could be

25 different for the past atmosphere (see sections 4.2, 4.4 and 4.5).

In this study, we report δ^{13}C-CH$_4$ offsets with respect to the conventional DI-IRMS measurement at NIWA (Lowe et al., 1991) because NIWA's δ^{13}C-CH$_4$ measurements have been compared with those from most laboratories to date (Table 1 and Fig. 1). In contrast, δD-CH$_4$ measurements from different laboratories have been limited. We report δD-CH$_4$ offsets of different laboratories with respect to the

5   IMAU measurement. The uncertainties presented in this study are generally standard errors of the mean, but numbers in the literature are cited as is. It should be therefore noted that the uncertainties, in particular those calculated by error propagation, are not rigorously consistent at all places in the manuscript.

5.1 NIWA

10   δ^{13}C-CH$_4$: As listed in Table 1, the DI-IRMS measurement at NIWA has been repeatedly intercompared with other laboratories. Importantly for this comparison, Bromley et al. (2012) reported the long-term stability of the measurement over the years 1992–2007, and it is likewise confirmed until 2011. The NIWA GC-IRMS system, based on the methodology of Miller et al. (2002), has an offset relative to the DI-IRMS of −0.19±0.26 ‰. Measurements on the GC-IRMS informing this instrument comparison are

15   subject to the Kr interference. A Kr-correction has since been derived in an empirical equation from the round robin intercomparison results (Schmitt et al., 2013 and section 4.4), accounting for differences in CH$_4$ mole fraction and an exponential fit to the GC-IRMS versus DI-IRMS results. The GC-IRMS system is currently equipped with a PCS column to eliminate the Kr interference.

5.2 IMAU

20   δ^{13}C-CH$_4$: According to Schmitt et al. (2013), the IMAU measurement at the present CH$_4$ mole fraction level is in agreement to NIWA with an offset value of −0.04±0.07 ‰ (No. 2 in Fig. 2a). This corresponds to the round robin comparison for the cylinder with CH$_4$ mole fraction of 1830.6 ppb (CA 03560) in Table 5 (section 4.4). The difference is −0.03±0.05 ‰ for data analyzed before the modification to remove the Kr interference (see Table 2 in Schmitt et al. (2013)). The intercomparison

25   in this study (section 3.4) also shows that the IMAU offset is −0.08±0.11 ‰ for the cylinder with the CH$_4$ mole fraction of 904.0 ppb (CA 71560).

δD-CH$_4$: As listed in Table 1, IMAU has made most intercomparisons with other laboratories so far. It is noted that the standard scale at IMAU was propagated from MPIC (Bergamaschi et al., 2000; section 2.2), and that it recently showed a reasonable agreement with the recent calibration at MPI-BGC (Sperlich et al., 2016).

5.3 MPIC

δ^{13}C-CH$_4$: As written in section 3.3, the standard scale at MPIC was transferred to IMAU (Brass and Röckmann, 2010; Sperlich et al., 2016). Since no direct comparison with NIWA is available, the MPIC offset relative to NIWA is estimated to be −0.04±0.07 ‰, identical to the IMAU offset (No. 3 in Fig. 2a).

δD-CH$_4$: Bock et al. (2010) reported an intercomparison using firn air samples between UB and MPIC, which indicated that, combined with the UB δD-CH$_4$ offset (section 5.14), the MPIC δD-CH$_4$ offset is +0.3±1.1 ‰ with respect to IMAU (No. 3 in Fig. 2b).

5.4 MPI-BGC

δ^{13}C-CH$_4$: Sperlich et al. (2016) quantified the offset of the IMAU standard scale relative to the primary standard scale at MPI-BGC. It was indicated that the MPI-BGC measurement differs by −0.03±0.10 ‰ from the IMAU standard scale. Combined with the IMAU offset relative to NIWA (section 5.2), the MPI-BGC offset is estimated to be −0.07±0.12 ‰ (No. 4 in Fig. 2a).

δD-CH$_4$: According to Sperlich et al. (2016), the MPI-BGC measurement is −4.2±1.2 ‰ from IMAU (No. 4 in Fig. 2b).

5.5 UCI

δ^{13}C-CH$_4$: Intercomparison exercises of UCI with external laboratories have been made several times. The oldest intercomparison (Lowe et al., 1991) reported good agreement (< 0.02 ‰) between the former UCI laboratory (S. Tyler at NCAR) and NIWA (INS, IGNS at that time). Among the later measurements, there are two direct intercomparisons with NIWA. (1) Tyler et al. (2007) reported an intercomparison result of UCI to be −0.01±0.09 ‰ with respect to NIWA (No. 5 left in Fig. 2a). For

this comparison, 16 air samples collected at Niwot Ridge, Colorado or Baring Head, New Zealand were exchanged between UCI and NIWA in 1998–1999. (2) This study (section 4.4 and Table 5) shows that the UCI measurement is +0.14±0.12 ‰ (No. 5 middle in Fig. 2a) and +0.04±0.08 ‰ higher than NIWA for the cylinders with high (CA 03560) and middle (CC 71560) CH_4 mole fractions, respectively. (3) In contrast, the intercomparison in this study (section 4.1 and Table 2) combined with the IMAU offset (section 5.2) yields +0.42±0.04 ‰ relative to NIWA (not shown in Fig. 2a), inconsistent with the above intercomparison results made earlier. The determinate error has yet to be resolved.

δD-CH_4: According to the intercomparison in this study (section 4.1), the UCI has a δD-CH_4 offset of −10.7±0.7 ‰ with respect to IMAU (No. 5 in Fig. 2b).

5.6 TU

δ^{13}C-CH_4: The intercomparison in this study (section 3.2) and the IMAU offset (section 5.2) give an offset of the TU measurements relative to NIWA to be +0.36±0.08 ‰ (No. 6 in Fig. 2b). Measurements at TU have been regularly compared with those at NIPR and they are in agreement within reproducibility of both systems (Umezawa et al., 2009 and additional measurements since then). This is consistent with the previous intercomparison between NIPR and NIWA (section 5.7) and indicates long-term intra-laboratory consistency of TU and NIPR measurements. It is reasonable that TU shares the offset level with NIPR, because both institutions use the same standard scale. As described in section 2.6, it should be noted that the above offset value is not for the datasets currently available to the research community (Umezawa et al., 2011, 2012a, 2012b), for which +0.32±0.08 ‰ (not shown in Fig. 2) is recommended. Correction of the datasets from the earlier publications is under evaluation.

δD-CH_4: The intercomparison in this study (section 4.2) gives an offset of −13.1±0.6 ‰ for the TU atmospheric δD-CH_4 measurement (No. 6 in Fig. 2b).

5.7 NIPR

δ^{13}C-CH_4: An intercomparison between NIPR and NIWA was conducted in 2004 (Morimoto et al., 2006). After the recent update of the NIPR standard scale, the NIPR offset is evaluated to be +0.33±0.04 ‰ higher than NIWA (No. 7 left in Fig. 2a). The intercomparison in this study (section 4.2)

combined with the IMAU offset (section 5.2) indicates the NIPR measurement is +0.27±0.08 ‰ with respect to NIWA (No. 7 right in Fig. 2a), consistent with the above value.

5.8 UW

δ^{13}C-CH$_4$: Quay et al. (1999) exchanged 30 air samples with NIWA; the average measurement offset was evaluated to be +0.02±0.14 ‰ (No. 8 left in Fig. 2a), although some individual samples disagreed by up to 0.5 ‰ (Lowe et al., 1994; Quay et al., 1999). Later, Levin et al. (2012) estimated that the UW offset is +0.058±0.004 ‰ with respect to NIWA based on co-located sampling at BHD (No. 8 right in Fig. 2a).

δD-CH$_4$: To our knowledge, no intercomparison exercises with UW have been reported.

5.9 UHEI

δ^{13}C-CH$_4$: Levin et al. (2012) estimated the UHEI δ^{13}C-CH$_4$ offset to be −0.169±0.031 ‰ relative to NIWA (No. 9 left in Fig. 2a). The intercomparison between UHEI and MPI-BGC in this study (section 3.3), together with the MPI-BGC offset (section 5.4), also infers the UHEI offset to be −0.05±0.13 ‰ (No. 9 right in Fig. 2a), consistent with the above value. Earlier measurements of three air samples at both UHEI and NIWA indicated that the UHEI offset is −0.04±0.04 ‰ relative to NIWA (Poß, 2003; Behrens et al., 2008). It is also noted that, in an intercomparison presented by Nisbet (2005), the UHEI measurement was −0.07±0.04 ‰ lower than NIWA. As these earlier comparison results have been published before the rigorous corrections of the UHEI measurements, these values are not included in Fig. 2a.

δD-CH$_4$: The intercomparison in this study (section 4.3), combined with the MPI-BGC offset (section 5.4), indicates that UHEI has an offset of −3.8±1.3 ‰ relative to IMAU.

5.10 INSTAAR

δ^{13}C-CH$_4$: Levin et al. (2012) estimated that the INSTAAR measurements have an offset of +0.132±0.022 ‰ with respect to NIWA (No. 10 left in Fig. 2a). In an intercomparison exercise reported by Nisbet (2005), the INSTAAR measurement was +0.14±0.06 ‰ higher than NIWA (not shown in Fig.

2a), consistent with the above value. This study (section 4.4) indicates that the INSTAAR measurement is +0.15±0.05 ‰ higher than NIWA for the cylinder with high CH_4 mole fraction (CA 03560) (No. 10 middle in Fig. 2a). The intercomparison between INSTAAR and MPI-BGC (section 4.5) indicates that, combined with the MPI-BGC offset (section 5.4), the INSTAAR offset is +0.21±0.12 ‰ relative to

5   NIWA (No. 10 second right in Fig. 2a). Lastly, the co-located sample intercomparison (section 4.6) indicates the INSTAAR offset to be +0.08±0.11 ‰ (No. 10 right in Fig. 2a). It is important to note again that only the round robin intercomparison measurements (section 4.4 and No. 10 middle in Fig. 2a) and the intercomparison with MPI-BGC (section 4.5) were made with a PCS column to remove the Kr interference, and that the dataset currently available to the public from INSTAAR will be evaluated

10   for future correction.

As described in section 2.10, INSTAAR follows the standard scale of UCI. Tyler et al. (2007) reported that measurements of 10 air cylinders filled at Niwot Ridge, Colorado in 2000–2001 were analyzed at both laboratories and that the result indicated an offset of INSTAAR to be +0.04±0.12 ‰ relative to UCI. The collection of air samples at Niwot Ridge for the UCI-INSTAAR comparison continued until

15   2003. A revisit to the measurement record showed that the INSTAAR offset relative to UCI had shifted over the years; the average differences are +0.02±0.08 ‰ for 2000 (N=7), +0.12±0.07 ‰ for 2001 (N=2) and +0.26±0.03 ‰ for 2002 (N=12). This fact may suggest excursions of the internal calibration of either laboratory for these years, but the cause has yet to be resolved; this problem will be addressed in a subsequent paper from either group. It is noted that the offsets relative to NIWA for both

20   laboratories inferred from the different intercomparison pathways are consistent with each other within the uncertainties (Figure 2a).

δD-CH_4: Bock et al. (2010) reported an intercomparison between UB and INSTAAR. This indicates that the INSTAAR measurement offset is −13.2±1.3 ‰ with respect to IMAU (No. 10 in Fig. 2b).

5.11 RHUL

25   δ^{13}C-CH_4: Nisbet (2005) reported that RHUL DI-IRMS measurements agreed well with NIWA with an offset of 0.00±0.02 ‰ (No. 11 left in Fig. 2a). At the same time, they indicated that the RHUL GC-IRMS measurement has an offset of +0.11±0.13 ‰ with respect to NIWA, and later Nisbet et al. (2016)

reported that the GC-IRMS system has an offset of about +0.3 ‰ relative to NIWA (not shown in Fig. 2a). Based on measurements of air in two cylinders exchanged between RHUL and NIWA in 2011 and 2014, RHUL applied an offset correction (−0.20 ‰) to all data (see section 4.6), by which the RHUL offset has now been evaluated to be +0.12±0.03 ‰ (No.11 middle in Fig. 2a). The intercomparisons based on the co-located air samples via INSTAAR (section 4.6), combined with the INSTAAR offset (section 5.10), infer that the RHUL offset is +0.10±0.03 ‰ relative to NIWA (No. 11 right in Fig. 2a).

5.12 PDX

δ^{13}C-CH$_4$: Rice et al. (2016) presented an offset of +0.024±0.088 ‰ of the PDX measurements relative to UW by comparing coinciding measurements of archive air samples at PDX and δ^{13}C-CH$_4$ records from Quay et al. (1999) from stations Mauna Loa, Hawaii and Tutuila, American Samoa (1995−1996). With the UW offset with respect to NIWA (section 5.8), it is indicated that the PDX measurement is +0.08±0.09 ‰ higher than NIWA (No. 12 in Fig. 2a). This offset is consistent with the UCI offset with respect to NIWA within the uncertainties (note that PDX follows the UCI standard scale).

δD-CH$_4$: Since PDX follows the UCI standard scale (Teama, 2013; Rice et al., 2016), the likely offset is same as that of UCI (No. 12 in Fig. 2b).

5.13 PSU

δ^{13}C-CH$_4$: According to Schmitt et al. (2013), the PSU measurement has an offset of +0.03±0.16 ‰ relative to NIWA after being corrected for the Kr interference. The measurements of the cylinder with high CH$_4$ mole fraction (CA 03560) at PSU are +0.03±0.16 ‰, +0.27±0.16 ‰ and +0.13±0.05 ‰ (No. 13 left, middle and right, respectively in Fig. 2a) higher than NIWA for different Kr corrections at different measurement times, these values being consistent with each other within the uncertainties.

δD-CH$_4$: An intercomparison result using three firn air samples gives the PSU offset of −12.1±1.5 ‰ relative to the IMAU measurement (Sapart et al., 2011; No. 13 left in Fig. 2b). The intercomparison in this study (section 4.4) gives −13.6±1.5 ‰ relative to IMAU for the cylinder with high CH$_4$ mole fraction (CA 03560) (No. 13 right in Fig. 2b).

5.14 UB

δ^{13}C-CH$_4$: The UB measurement has an offset of −0.18±0.09‰ relative to NIWA (Schmitt et al., 2013; No. 14 in Fig. 2a). This was determined by the round robin intercomparison (section 4.4 and Table 5).

δD-CH$_4$: Sapart et al. (2011) gives an intercomparison result between UB and IMAU, indicating the UB
5   offset of 0.0±1.6 ‰ relative to IMAU (No. 14 left in Fig. 2b). This value is consistent with the intercomparisons between UB and IMAU reported by Bock et al. (2010). Later UB modified the measurement set up, but the measurements of same air samples before and after all modifications were in good agreement as presented by Bock et al. (2014). The intercomparison in this study (section 3.4) shows that the UB measurement differs insignificantly by −0.8±2.5 ‰ with respect to IMAU for the
10   cylinder with high CH$_4$ mole fraction (CA 03560) (No. 14 right in Fig. 2b).

5.15 AWI

δ^{13}C-CH$_4$: The AWI offset is reported to be −0.09±0.06‰ with respect to NIWA (Schmitt et al., 2013; No. 15 in Fig. 2a).

5.16 CIC

15   δ^{13}C-CH$_4$: Sperlich et al. (2012) reported measurements of an air cylinder at CIC, IMAU and UB. The CIC measurement insignificantly different by +0.01±0.09 ‰ from IMAU, and the CIC offset with respect to NIWA is estimated to be −0.03±0.11 (No. 16 left in Fig. 2a). They have also reported that the CIC measurement is in agreement with UB with difference of +0.00±0.14 ‰. It is noted that, although the UB offset relative to NIWA is estimated to be significant (section 5.14), the difference is still within
20   uncertainties of the intercomparison exercises. Two pure CH$_4$ gases prepared by Sperlich et al. (2012) constitute crucial components of the reference gas series developed at MPI-BGC (Sperlich et al., 2016). This has provided a direct intercomparison between CIC and MPI-BGC. The CIC measurement is +0.09±0.14 ‰ higher than MPI-BGC. Combined with the MPI-BGC offset (section 5.4), the CIC offset with respect to NIWA is estimated to be +0.02±0.18 ‰ (No. 16 right in Fig. 2a), consistent with the
25   aforementioned value.

δD-CH$_4$: Sperlich et al. (2016) reported δD-CH$_4$ measurement results of the two reference gases prepared by Sperlich et al. (2012) at CIC and MPI-BGC. The results indicated that the CIC measurement differs by +2.1±1.8 ‰ from MPI-BGC. Combined with the MPI-BGC offset (section 4.4), the CIC offset relative to IMAU is estimated to be −2.1±2.1 ‰ (No. 16 in Fig. 2b).

6 Summary and Discussion

We carried out inter-laboratory comparison exercises for atmospheric δ^{13}C-CH$_4$ and δD-CH$_4$ covering many laboratories around the world. In addition, we reviewed previously published intercomparison results. The results indicated measurement offsets among laboratories, which range from −0.2 to +0.3 ‰ with respect to the NIWA DI-IRMS measurement for δ^{13}C-CH$_4$ and up to −13 ‰ with respect to the IMAU measurement for δD-CH$_4$. These offset values are larger than measurement uncertainties of individual laboratories.

The significant δ^{13}C-CH$_4$ measurement offsets among laboratories are obvious even though all laboratories ultimately reference to the VPDB scale. We have presented potential causes of the measurement offsets in individual laboratories (section 2), with possible further causes being hidden in all preparation and measurement steps of standard materials. (1) The scale contraction effect for DI-IRMS CO$_2$ analysis, which is instrument-dependent, could be responsible for considerable part of the observed offsets, given the fact that the atmospheric δ^{13}C-CH$_4$ value (about −47 ‰) differs considerably from the primary anchor of the VPDB scale (NBS-19). (2) Individual laboratories have made calibrations against different RMs with different uncertainties of assigned values; such diverse calibration trajectories have also definitely contributed to the inter-laboratory measurement offsets. Such RMs have different chemical properties and are processed to CO$_2$ at individual laboratories, in which different fractionation is possible. (3) Different algorithms for ^{17}O correction have been used for δ^{13}C measurements at different laboratories, which could have caused biases among available datasets. (4) The Kr interference on a GC-IRMS system is in several cases a probable cause of the offsets and unfortunately, this effect is system-dependent and can vary with time, depending on the instrument settings. Lastly, it is important to note that we summarized δ^{13}C-CH$_4$ measurement offsets at the

modern atmospheric CH_4 mole fraction level, but the offset may vary with the amount of CH_4 analyzed (e.g. lower mole fractions in ice core analyses, see Table 3, 5 and 6), because of a non-linear response of IRMS (Umezawa et al., 2009) and because of the Kr interference is directly dependent on the Kr to CH_4 ratio (Schmitt et al., 2013). Furthermore, the intercomparisons presented here focus on modern

5   atmospheric CH_4 of typically −47 ‰ and such comparisons for high and low $\delta^{13}C$-CH_4 values (e.g. CH_4 from ice cores or enriched/depleted source signatures) are to date very limited (Tables 3 and 6 in this study).

Concerning δD-CH_4 measurement offsets among laboratories, it is interesting that the listed laboratories can be roughly split into two groups whose δD-CH_4 measurements differ by ~10 ‰. Some laboratories

10   with higher δD-CH_4 values reference to an identical set of standards produced at MPIC (MPIC and IMAU) or to the UHEI calibration (UHEI and UB), and measurements of these groups have been cross-referenced (see sections 2 and 4), thereby showing the reasonable agreements. The original calibrations were made by an offline CH_4 processing technique (cryogenic separation and conversion of CH_4 to CO_2 and H_2O followed by H_2O reduction to H_2) with subsequent analysis by DI-IRMS. The other

15   laboratories with higher δD-CH_4 values recently developed their own primary calibrations independently (CIC and MPI-BGC). CIC used an offline CH_4 processing combined with DI-IRMS, whereas MPI-BGC adopted TC/EA coupled to continuous-flow IRMS. For the lower δD-CH_4 group, some laboratories made calibrations against Oztech H_2 gases (UCI, PDX and PSU) or have other calibration pathways (TU and INSTAAR) (see section 2). These laboratories used local H_2 working gas

20   standards for GC-IRMS, which were calibrated by a separate DI-IRMS procedure. As is the case for $\delta^{13}C$-CH_4, possible causes of the observed δD-CH_4 discrepancies could have arisen in all preparation and measurement steps. (1) The classical technique for DI-IRMS involves processing of H_2O, and the associated steps in experimental lines are prone to surface adhesion and contamination of H_2O, thereby considerable memory effect is possible (Bergmaschi et al., 2000). (2) Similar to $\delta^{13}C$-CH_4, calibration

25   for δD-CH_4 involves measurements of standards with different chemical properties (H_2O and H_2), and such calibrations at different laboratories could contribute to the offset. (3) Difficulties in maintaining stable pyrolysis conditions for GC-IRMS (Bock et al. 2010) might have affected measurements against local H_2 working standards in the cases where the principle of identical treatment (Werner and Brand,

2001) was not followed strictly. Lastly, it is noted that non-linearity of the IRMS in δD-CH$_4$ measurements (Brass and Röckmann, 2010) may also play a role for samples with low mole fractions such as ice core analyses.

The measurement offsets summarized in this study should be thoroughly taken into account when data from different laboratories are combined, and this study will be of help when incorporating merged δ^{13}C-CH$_4$ and δD-CH$_4$ datasets into a state-of-the-art chemistry transport model. However it is recommended that data users contact the data providers directly for the latest information whenever possible. The Kr interference is under evaluation at some laboratories and it will possibly involve an update of the datasets currently available. More importantly, it is imperative to have common reference gases with transparent and reproducible traceability (for instance, Sperlich et al. 2016) and to carry out a systematic intercomparison program (flask or cylinder round robin) in the research community for attaining the necessary but ambitious high compatibility goals of 0.02 ‰ for δ^{13}C-CH$_4$ and 1 ‰ for δD-CH$_4$ (WMO, 2016). Such thorough efforts will facilitate optimized use of δ^{13}C-CH$_4$ and δD-CH$_4$ datasets in a combined way and maximize the number of isotope datasets (and thus their spatial and temporal coverage) usable for enhancing our understanding of the global CH$_4$ cycle.

We welcome collaborative works to analyse the multiple datasets presented in this study (see data availability listed in Table 1). Data users can examine the offset numbers (Table 1 and Figure 2) to adjust the datasets at least for data points with values close to the modern atmosphere in δ^{13}C-CH$_4$ and δD-CH$_4$ as well as CH$_4$ mole fraction. For data with CH$_4$ mole fractions and isotopic ratios that are far from modern background values (e.g. sample air from ice core and stratosphere and those influenced by sources), more intercomparisons are needed to establish correction factors among datasets.

List of Participating Institution/Project Acronyms

AWI: Alfred Wegener Institute Helmholtz Centre for Polar and Marine Research, Bremerhaven, Germany

CARIBIC: Civil Aircraft for the Regular Investigation of the atmosphere Based on an Instrument Container

CIC: Center for Ice and Climate, Niels Bohr Institute, University of Copenhagen, Copenhagen, Denmark

IMAU: Institute for Marine and Atmospheric research Utrecht, Utrecht University, Utrecht, the Netherlands

5 INSTAAR: Institute of Arctic and Alpine Research University of Colorado Boulder, Boulder, USA

MPI-BGC: Max Planck Institute for Biogeochemistry, Jena, Germany

MPIC: Max Planck Institute for Chemistry, Mainz, Germany

NCAR: National Center for Atmospheric Research, Boulder, USA

NIPR: National Institute of Polar Research, Tokyo, Japan

10 NIWA: National Institute for Water and Atmospheric Research, Wellington, New Zealand

NOAA: National Oceanic and Atmospheric Administration, USA

PDX: Portland State University, Portland, USA

PSU: Pennsylvania State University, Pennsylvania, USA

RHUL: Royall Holloway, University of London, Egham, UK

15 TU: Tohoku University, Sendai, Japan

UB: University of Bern, Bern, Switzerland

UCI: University of California Irvine, Irvine, USA

UHEI: University of Heidelberg, Heidelberg, Germany

UW: University of Washington, Seattle, USA

20 **Acknowledgement**

We thank M. Sato for measurements at TU. We thank Owen Sherwood for contribution to setting up the INSTAAR measurement system, and Ken Masarie and John Mund, who developed software enabling data comparisons from co-located samples measured by INSTAAR, RHUL and NIWA. We thank Paul Quay (UW) for isotopic CH_4 data and intercalibration information and Doaa Teama for isotopic

25 measurements at PDX. We thank C. Sapart for helpful information about the past intercomparison. Part of this work at NIES was supported by the Environment Research and Technology Development Fund (2-1710) of the Ministry of the Environment, Japan and Environmental Restoration and Conservation

Agency. Funding for work at PDX was provided by the US National Science Foundation (Atmospheric and Geospace Sciences Grant 0952307). CH_4 isotope ice core work at UB received funding from the European Research Council under the European Union's Seventh Framework Programme (FP7/2007-2013) ERC grant agreement no 226172 and the Swiss National Science Foundation (grant no 200020_159563 & 20020_172506). NIWA's isotope measurements are funded under the Climate and Atmosphere Research Programme CAAC1804 (2017/18 SCI).

References

Allison, C. E., Francey, R. J., and Meijer H. A. J.: Recommendations for the reporting of stable isotope measurements of carbon and oxygen in CO_2 gas, TECDOC-825 IAEA, Vienna, 1995, 155–162.

Aoki, S., Nakazawa, T., Murayama, S. and Kawaguchi, S.: Measurements of atmospheric methane at the Japanese Antarctic Station, Syowa, Tellus, 44B, 273–281, 1992.

Assonov, S. S., and Brenninkmeijer, C. A. M.: On the ^{17}O correction for CO_2 mass spectrometric isotopic analysis, Rapid Commun. Mass Sp., 17, 1007–1016, doi:10.1002/rcm.1012, 2003.

Behrens, M., Schmitt, J., Richter, K.-U., Bock, M., Richter, U., Levin, I., and Fischer, H.: A gas chromatography/combustion/isotope ratio mass spectrometry system for high-precision $\delta^{13}C$ measurements of atmospheric methane extracted from ice core samples, Rapid Commun. Mass Sp., 22, 3261–3269, doi:10.1002/rcm.3720, 2008.

Bergamaschi, P., Schupp, M., and Harris, G. W.: High-precision direct measurements of $^{13}CH_4/^{12}CH_4$ and $^{12}CH_3D/^{12}CH_4$ ratios in atmospheric methane sources by means of a long-path tunable diode laser absorption spectrometer, Appl. Opt., 33(33), 7704–7716, 1994.

Bergamaschi, P., Bräunlich, M., Marik, T., and Brenninkmeijer, C. A. M.: Measurements of the carbon and hydrogen isotopes of atmospheric methane at Izana, Tenerife: Seasonal cycles and synoptic-scale variations, J. Geophys. Res.-Atmos., 105, 14531–14546, doi:10.1029/1999JD901176, 2000.

Bock, M., Schmitt, J., Behrens, M., Möller, L., Schneider, R., Sapart, C., and Fischer, H.: A gas chromatography/pyrolysis/isotope ratio mass spectrometry system for high- precision δD measurements

of atmospheric methane extracted from ice cores, Rapid Commun. Mass Sp., 24, 621–633, doi:10.1002/rcm.4429, 2010.

Bock, M., Schmitt, J., Beck, J., Schneider, R. and Fischer H.: Improving accuracy and precision of ice core $\delta D(CH_4)$ analyses using methane pre-pyrolysis and hydrogen post-pyrolysis trapping and

5 subsequent chromatographic separation, Atmos. Meas. Tech., 7, 1999–2012, doi:10.5194/amt-7-1999-2014, 2014.

Bock, M., Schmitt, J., Beck, J., Seth, B., Chappellaz, J., Fischer, H.: Glacial/interglacial wetland, biomass burning, and geologic methane emissions constrained by dual stable isotopic CH_4 ice core records, PNAS, E5778–E5786, doi:10.1073/pnas.1613883114, 2017.

10 Brand, W., Coplen, T. B., Vogl, J., Rosner, M., and Prohaska, T.: Assessment of international reference materials for isotope-ratio analysis (IUPAC Technical Report), Pure Applied Chem., 86(3), 425–467, doi:10.1515/pac-2013-1023, 2014.

Brand, W., Rothe, M., Sperlich, P., Strube, M., and Wendeberg M.: Automated simultaneous measurement of the $\delta^{13}C$ and δ^2H values of methane and the $\delta^{13}C$ and $\delta^{18}O$ values of carbon dioxide in

15 flask samples using a new multi cryo-trap/gas chromatography/isotope ratio mass spectrometry system, Rapid Commun. Mass Spectrom., 30, 1523–1539, doi:10.1002/rcm.7587, 2016.

Brass, M. and Röckmann, T.: Continuous-flow isotope ratio mass spectrometry method for carbon and hydrogen isotope measurements on atmospheric methane, Atmos. Meas. Tech., 3, 1707–1721, doi:10.5194/amt-3-1707-2010, 2010.

20 Bräunlich, M., Aballanin, O., Marik, T., Jockel, P., Brenninkmeijer, C. A. M., Chappellaz, J., Barnola, J. M., Mulvaney, R., and Sturges, W. T.: Changes in the global atmospheric methane bud- get over the last decades inferred from 13C and D isotopic analysis of Antarctic firn air, J. Geophys. Res.-Atmos., 106, 20465–20481, doi:10.1029/2001JD900190, 2001.

Brenninkmeijer, C. A. M., Crutzen, P. J., Fischer, H., Gusten, H., Hans, W., Heinrich, G., Heintzenberg,

25 J., Hermann, M., Immelmann, T., Kersting, D., Maiss, M., Nolle, M., Pitscheider, A., Pohlkamp, H., Scharffe, D., Specht, K., and Wiedensohler, A.: CARIBIC – Civil aircraft for global measurement of

trace gases and aerosols in the tropopause region, J. Atmos. Oceanic Technol., 16, 1373−1383, doi: 10.1175/1520- 0426(1999)016<1373:Ccafgm>2.0.Co;2, 1999.

Bromley, T., Allan, W., Martin, R., Mikaloff Fletcher, S. E., Lowe, D. C., Struthers, H., and Moss, R.: Shipboard measurements and modeling of the distribution of CH_4 and $^{13}CH_4$ in the western Pacific, J. Geophys. Res., 117, D04307, doi:10.1029/2011JD016494, 2012.

Burgoyne, T. W., and Hayes J. M.: Quantitative production of H_2 by Pyrolysis of gas chromatographic effluents, Anal. Chem., 70, 24, 5136–5141, doi:10.1021/ac980248v, 1998.

Coplen, T. B., Brand, W. A., Gehre, M., Gröning, M., Meijer, H. A. J., Toman, B., and Verkouteren, R. M.: New guidelines for $\delta^{13}C$ measurements, Anal. Chem., 78(7), 2439–2441, doi:10.1021/ac052027c, 2006.

Craig, H.: Isotopic standards for carbon and oxygen and correction factors for mass-spectrometric analysis of carbon dioxide, Geochim. Cosmochim. Acta, 12, 133, doi: 10.1016/0016-7037(57)90024-8, 1957.

Dlugokencky, E. J., Myers, R. C., Lang, P. M., Masarie, K. A., Crotwell, A. M., Thoning, K. W., Hall, B. D., Elkins, J. W., and Steele, L. P.: Conversion of NOAA atmospheric dry air CH_4 mole fractions to a gravimetrically prepared standard scale, J. Geophys. Res., 110, D18306, doi:10.1029/2005JD006035, 2005.

Eyer, S., Tuzson, B., Popa, M. E., van der Veen, C., Röckmann, T., Rothe, M., Brand, W. A., Fisher, R., Lowry, D., Nisbet, E. G., Brennwald, M. S., Harris, E., Zellweger, C., Emmenegger, L., Fischer, H., and Mohn, J.: Real-time analysis of $\delta^{13}C$- and δD-CH_4 in ambient air with laser spectroscopy: method development and first intercomparison results, Atmos. Meas. Tech., 9, 263-280, https://doi.org/10.5194/amt-9-263-2016, 2016.

Ferretti, D. F., Miller, J. B., White, J. W. C., Etheridge, D. M., Lassey, K. R., Lowe, D. C., MacFarling Meure, C. M., Dreier, M. F., C. M. Trudinger, C. M., van Ommen, T. D., and Langenfelds, R. L.: Unexpected changes to the global methane budget over the past 2000 years, Science, 309, 1714–1717, doi: 10.1126/science.1115193, 2005.

Fischer, H., Behrens, M., Bock, M., Richter, U., Schmitt, J., Loulergue, L., Chappellaz, J., Spahni, R., Blunier, T., Leuenberger, M., and Stocker, T. F.: Changing boreal methane sources and constant biomass burning during the last termination, Nature, 452, 864–867, doi:10.1038/nature06825, 2008.

Fisher, R., Lowry, D., Wilkin, O., Sriskantharajah, S., and Nisbet, E. G.: High-precision, automated stable isotope analysis of atmospheric methane and carbon dioxide using continuous-flow isotope-ratio mass spectrometry, Rapid Commun. Mass Spectrom., 20(2), 200–208, doi:10.1002/rcm.2300, 2006.

Fisher, R. E., Sriskantharajah, S., Lowry, D., Lanoisellé, M., Fowler, C. M. R., James, R. H., Hermansen, O., Lund Myhre, C., Stohl, A., Greinert, J., Nisbet-Jones, P. B. R., Mienert, J., and Nisbet, E. G.: Arctic methane sources: Isotopic evidence for atmospheric inputs, Geophys. Res. Lett., 38, L21803, doi:10.1029/ 2011GL049319, 2011.

Fung, I., John, J., Lerner, J., Matthews, E., Prather, M., Steele, L. P., and Fraser, P. J.: Three-dimensional model synthesis of the global methane cycle, J. Geophys. Res., 96(D7), 13033–13065, doi:10.1029/91JD01247, 1991.

Ghosh, A., Patra, P. K., Ishijima, K., Umezawa, T., Ito, A., Etheridge, D. M., Sugawara, S., Kawamura, K., Miller, J. B., Dlugokencky, E. J., Krummel, P. B., Fraser, P. J., Steele, L. P., Langenfelds, R. L., Trudinger, C. M., White, J. W. C., Vaughn, B., Saeki, T., Aoki, S., and Nakazawa, T.: Variations in global methane sources and sinks during 1910–2010, Atmos. Chem. Phys., 15, 2595-2612, doi:10.5194/acp-15-2595-2015, 2015.

Hein, R., Crutzen, P. J., and Heimann, M.: An inverse modeling approach to investigate the global atmospheric methane cycle, Global Biogeochem. Cycles, 11, 43–76, doi:10.1029/96GB03043, 1997.

Hilkert, A. W., Douthitt, C. B., Schlüter, H. J., and Brand W. A.: Isotope ratio monitoring gas chromatography/mass Spectrometry of D/H by high temperature conversion isotope ratio mass spectrometry, Rapid Comm. Mass Spec., 13, 1226–1230, doi:10.1002/(SICI)1097-0231(19990715)13:13<1226::AID-RCM575>3.0.CO;2-9, 1999.

Kai, F. M., Tyler, S. C., Randerson, J. T., and Blake, D. R.: Reduced methane growth rate explained by decreased Northern Hemisphere microbial sources, Nature, 476, 194–197, doi:10.1038/nature10259, 2011.

Kirschke, S., Bousquet, P., Ciais, P., Saunois, M., Canadell, J. G., Dlugokencky, E. J., Bergamaschi, P., Bergmann, D., Blake, D. R., Bruhwiler, L., Cameron-Smith, P., Castaldi, S., Chevallier, F., Feng, L., Fraser, A., Heimann, M., Hodson, E. L., Houweling, S., Josse, B., Fraser, P. J., Krummel, P. B., Lamarque, J.-F., Langenfelds, R. L., Le Quéré, C., Naik, V., O'Doherty, S., Palmer, P. I., Pison, I., Plummer, D., Poulter, B., Prinn, R. G., Rigby, M., Ringeval, B., Santini, M., Schmidt, M., Shindell, D. T., Simpson, I. J., Spahni, R., Steele, L. P., Strode, S. A., Sudo, K., Szopa, S., van der Werf, G. R., Voulgarakis, A., van Weele, M., Weiss, R. F., Williams, J. E., and Zeng, G.: Three decades of global methane sources and sinks, Nature Geoscience, 6, 813–823, doi:10.1038/ngeo1955, 2013.

Levin, I., Bergamaschi, P., Dörr, H., and Trapp, D.: Stable isotopic signature of methane from major sources in Germany, Chemosphere, 26, 1–4, 161–177, doi:10.1016/0045-6535(93)90419-6, 1993.

Levin, I., Glatzel-Mattheier, H., Marik, T., Cuntz, M., and Schmidt, M.: Verification of German methane emission inventories and their recent changes based on atmospheric observations, J. Geophys. Res., 104, D3, 3447–3456, doi:10.1029/1998JD100064, 1999.

Levin, I., Veidt, C., Vaughn, B. H., Brailsford, G., Bromley, T., Heinz, R., Lowe, D., Miller, J. B., Poss, C., and White, J. W. C.: No inter-hemispheric $\delta^{13}CH_4$ trend observed, Nature, 486, E3–E4, doi:10.1038/nature11175, 2012.

Lowe, D. C., Brenninkmeijer, C. A. M., Manning M. R., Sparks, R., and Wallace, G.: Radiocarbon determination of atmospheric methane at Baring Head, New Zealand, Nature, 332, 522–525, doi:10.1038/332522a0, 1988.

Lowe, D. C., Brenninkmeijer, C. A. M., Tyler, S. C., and Dlugkencky, E. J.: Determination of the Isotopic Composition of Atmospheric Methane and its Application in the Antarctic, J. Geophys. Res.-Atmos., 96, 15455–15467, doi:10.1029/91JD01119, 1991.

Lowe, D. C., Brenninkmeijer, C. A. M., Brailsford, G. W., Lassey, K. R., and Gomez, A. J.: Concentration and ^{13}C records of atmospheric methane in New Zealand and Antarctica: Evidence for changes in methane sources, J. Geophys. Res., 99, D8, 16913–16925, doi:10.1029/94JD00908, 1994.

Lowe, D. C., Manning, M. R., Brailsford, G., and Bromley, A. M.: The 1991–1992 atmospheric methane anomaly: Southern Hemisphere ^{13}C decrease and growth rate fluctuations, Geophys. Res. Lett., 24, 8, 857–860, doi:10.1029/97GL00830, 1997.

Lowe, D. C., Allan, W., Manning, M. R., Bromley, T., Brailsford, G., Ferretti, D., Gomez, A., Knobben, R., Martin, R., Mei, Z., Moss, R., Koshy, K., and Maata, M.: Shipboard determinations of the distribution of C-13 in atmospheric methane in the Pacific, J. Geophys. Res.-Atmos., 104, 26125–26135, doi:10.1029/1999jd900452, 1999.

Lowe, D. C., Koshy, K., Bromley, T., Allan, W., Struthers, H., Mani, F., and Maata, M.: Seasonal cycles of mixing ratio and ^{13}C in atmospheric methane at Suva, Fiji, J. Geophys. Res., 109, D23308, doi:10.1029/2004JD005166, 2004.

Lowry, D., Holmes, C. W., Rata, N. D., O'Brien, P., and Nisbet, E. G.: London methane emissions: Use of diurnal changes in concentration and δ^{13}C to identify urban sources and verify inventories, J. Geophys. Res., 106(D7), 7427–7448, doi:10.1029/2000JD900601, 2001.

Meijer, H. A. J., Neubert, R. E. M., and Visser, G. H.: Cross contamination in dual inlet isotope ratio mass spectrometers, Int. J. Mass Spectrom., 198, 45–61, 2000.

Merritt, D. A., Hayes, J. M., and Des Marais, D. J.: Carbon isotopic analysis of atmospheric methane by isotope-ratio-monitoring gas-chromatography mass-spectrometry, J. Geophys. Res., 100, D1, 1317–1326, doi:10.1029/94JD02689, 1995.

Mikaloff Fletcher, S. E., Tans, P. P., Bruhwiler, L. M., Miller, J. B., and Heimann, M.: CH$_4$ sources estimated from atmospheric observations of CH$_4$ and its ^{13}C/^{12}C isotopic ratios: 1.Inverse modeling of source processes, Global Biogeochem. Cy., 18, GB4004, doi:10.1029/2004GB002223, 2004a.

Mikaloff Fletcher, S. E., Tans, P. P., Bruhwiler, L. M., Miller, J. B., and Heimann, M.: CH$_4$ sources estimated from atmospheric observations of CH$_4$ and its ^{13}C/^{12}C isotopic ratios: 2. Inverse modeling of

CH4 fluxes from geographical regions, Global Biogeochem. Cy., 18, GB4005, doi:10.1029/2004GB002224, 2004b.

Miller, J. B., Mack, K. A., Dissly, R., White, J. W. C., Dlugokencky, E. J., and Tans, P. P.: Development of analytical methods and measurements of $\delta^{13}C$ in atmospheric CH_4 from the NOAA/CMDL global air sampling network, J. Geophys. Res., 107, 4178, doi:10.1029/2001JD000630, 2002.

Möller, L., Sowers, T., Bock, M., Spahni R., Behrens, M., Schmitt, J., Miller, H., and Fischer, H.: Independent variations of CH_4 emissions and isotopic composition over the past 160,000 years, Nature Geoscience, 6, 885–890, doi:10.1038/NGEO1922, 2013.

Monteil, G., Houweling, S., Dlugockenky, E. J., Maenhout, G., Vaughn, B. H., White, J. W. C., and Röckmann, T.: Interpreting methane variations in the past two decades using measurements of CH_4 mixing ratio and isotopic composition, Atmos. Chem. Phys., 11, 9141–9153, doi:10.5194/acp-11-9141-2011, 2011.

Morimoto, S., Aoki, S., Nakazawa, T., and Yamanouchi, T.: Temporal variations of the carbon isotopic ratio of atmospheric methane observed at Ny Ålesund, Svalbard from 1996 to 2004,Geophys. Res. Lett., 33, L01807, doi:10.1029/2005GL024648, 2006.

Nisbet, E. (Ed.), Meth-MonitEUr: Methane Monitoring in the Euro- pean Union and Russia, Eur. Comm., Brussels, 2005.

Nisbet, E. G., E. J. Dlugokencky, M. R. Manning, D. Lowry, R. E. Fisher, J. L. France, S. E. Michel, J. B. Miller, J. W. C. White, B. Vaughn, P. Bousquet, J. A. Pyle, N. J. Warwick, M. Cain, R. Brownlow1, G. Zazzeri, M. Lanoisellé, A. C. Manning, E. Gloor, D. E. J. Worthy, E.-G. Brunke, C. Labuschagne, E. W. Wolff, and A. L. Ganesan, Rising atmospheric methane: 2007–2014 growth and isotopic shift, Global Biogeochem. Cy., 30, doi:10.1002/ 2016GB005406, 2016.

Poß, C.: Investigation of the variability of atmospheric methane in polar regions based on trajectory analysis and the measurement of stable isotopes (in German), PhD thesis, Heidelberg University, 2003.

Quay, P. D., King, S. L., Stutsman, J., Wilbur, D. O., Steele, L. P., Fung, I., Gammon, R. H., Brown, T. A., Farwell, G. W., Grootes, P. M., and Schmidt, F. H.: Carbon isotopic composition of atmospheric CH4: Fossil and biomass burning strengths, Global Biogeochem. Cy., 5, 25–47, 1991.

Quay, P., Stutsman, J., Wilbur, D., Snover, A., Dlugokencky, E., and Brown, T.: The isotopic composition of atmospheric methane, Global Biogeochem. Cy., 13, 445–461, 1999.

Rice, A. L., Gotoh, A. A., Ajie, H. O., and Tyler, S. C.: High-precision continuous-flow measurement of δ^{13}C and δD of atmospheric CH4, Anal. Chem., 73, 4104–4110, doi:10.1021/ac0155106, 2001.

Rice, A. L., C. L. Butenhoff, D. G. Teama, F. H. Röger, M. A. K. Khalil, and R. A. Rasmussen, Atmospheric methane isotopic record favors fossil sources flat in 1980s and 1990s with recent increase, Proc. Natl. Acad. Sci., 113, 39, 10791–10796, doi:10.1073/pnas.1522923113, 2016.

Rigby, M., Montzka, S. A., Prinn, R. G., White, J. W. C., Young, D., O'Doherty, S., Lunta, M. F., Ganesan, A. L., Manning, A. J., Simmonds, P. G., Salameh, P. K., Harth, C. M., Mühle, J., Weiss, R. F., Fraser, P. J., L. Steele, P. Krummel, P. B., McCulloch, A., and Park, S.: Role of atmospheric oxidation in recent methane growth, Proc. Natl. Acad. Sci., 114, 21, 5373–5377, doi: 10.1073/pnas.1616426114, 2017.

Röckmann, T.: Measurement and interpretation of ^{13}C, ^{14}C, ^{17}O and ^{18}O variations in atmospheric carbon monoxide, Ph.D. thesis, Univ. Heidelberg, Heidelberg, Germany, 1998.

Röckmann, T., Brass, M., Borchers, R., and Engel, A.: The isotopic composition of methane in the stratosphere: high-altitude balloon sample measurements, Atmos. Chem. Phys., 11, 13287-13304, https://doi.org/10.5194/acp-11-13287-2011, 2011.

Röckmann, T., Eyer, S., van der Veen, C., Popa, M. E., Tuzson, B., Monteil, G., Houweling, S., Harris, E., Brunner, D., Fischer, H., Zazzeri, G., Lowry, D., Nisbet, E. G., Brand, W. A., Necki, J. M., Emmenegger, L., and Mohn, J.: In situ observations of the isotopic composition of methane at the Cabauw tall tower site, Atmos. Chem. Phys., 16, 10469-10487, doi:10.5194/acp-16-10469-2016, 2016.

Santrock J, Studley, S. A, Hayes J. M.: Isotopic analyses based on the mass spectra of carbon dioxide, Anal. Chem., 57, 1444, doi: 10.1021/ac00284a060, 1985.

Sapart, C. J., van der Veen, C., Vigano, I., Brass, M., van de Wal, R. S. W., Bock, M., Fischer, H., Sowers, T., Buizert, C., Sperlich, P., Blunier, T., Behrens, M., Schmitt, J., Seth, B., and Röckmann, T.: Simultaneous stable isotope analysis of methane and nitrous oxide on ice core samples, Atmos. Meas. Tech., 4, 2607–2618, doi:10.5194/amt-4-2607-2011, 2011.

Sapart, C. J., Monteil, G., Prokopiou, M., van de Wal, R. S. W., Kaplan, J. O., Sperlich, P., Krumhardt, K. M., van der Veen, C., Houweling, S., Krol, M. C., Blunier, T., Sowers, T., Martinerie, P., Witrant, E., Dahl-Jensen, D. and Röckmann, T: Natural and anthropogenic variations in methane sources during the past two millennia, Nature, 490, 85–88, doi:10.1038/nature11461, 2012.

Sapart, C. J., Martinerie, P., Witrant, E., Chappellaz, J., van de Wal, R. S. W., Sperlich, P., van der Veen, C., Bernard, S., Sturges, W. T., Blunier, T., Schwander, J., Etheridge, D., and Röckmann, T.: Can the carbon isotopic composition of methane be reconstructed from multi-site firn air measurements?, Atmos. Chem. Phys., 13, 6993-7005, https://doi.org/10.5194/acp-13-6993-2013, 2013.

Schaefer, H., S. E. Mikaloff Fletcher, C. Veidt, K. R. Lassey, G. W. Brailsford, T. M. Bromley, E. J. Dlugokencky, S. E. Michel, J. B. Miller, I. Levin, D. C. Lowe, R. J. Martin, B. H. Vaughn, J. W. C. White: A 21st-century shift from fossil-fuel to biogenic methane emissions indicated by [13]CH$_4$, Science, 352 (6281), 80–84, doi:10.1126/science.aad2705, 2016.

Schmitt, J., Seth, B., Bock, M., van der Veen, C., Möller, L., Sapart, C. J., Prokopiou, M., Sowers, T., Röckmann, T., and Fischer, H.: On the interference of Kr during carbon isotope analysis of methane using continuous-flow combustion–isotope ratio mass spectrometry, Atmos. Meas. Tech., 6, 1425-1445, doi:10.5194/amt-6-1425-2013, 2013.

Schmitt, J., Seth, B., Bock, M., and Fischer, H.: Online technique for isotope and mixing ratios of CH$_4$, N$_2$O, Xe and mixing ratios of organic trace gases on a single ice core sample, Atmos. Meas. Tech., 7, 2645–2665, doi:10.5194/amt-7-2645-2014, 2014.

Schwietzke, S., O. A. Sherwood, L. M. P. Bruhwiler, J. B. Miller, G. Etiope, E. J. Dlugokencky, S. E. Michel, V. A. Arling, B. H. Vaughn, J. W. C. White and P. P. Tans, Upward revision of global fossil fuel methane emissions based on isotope database, Nature, 538, 88–91, doi:10.1038/nature19797, 2016.

Sherwood, O. A., Schwietzke, S., Arling, V. A., and Etiope, G.: Global Inventory of Gas Geochemistry Data from Fossil Fuel, Microbial and Burning Sources, version 2017, Earth Syst. Sci. Data, 9, 639-656, doi:10.5194/essd-9-639-2017, 2017.

Sowers, T.: Late Quaternary atmospheric CH_4 isotope record suggests marine clathrates are stable, Science, 311, 5762, 838–840, doi:10.1126/science.1121235, 2006.

Sowers, T.: Atmospheric methane isotope records covering the Holocene period, Quaternary Sci. Rev., 29, 213–221, doi:10.1016/j.quascirev.2009.05.023, 2010.

Sowers, T., Bernard, S., Aballain, O., Chappellaz, J., Barnola, J. M., and Marik, T.: Records of the $\delta^{13}C$ of atmospheric CH_4 over the last 2 centuries as recorded in Antarctic snow and ice, Global Biogeochem. Cy., 19, GB2002, doi:10.1029/2004GB002408, 2005.

Sperlich, P., Guillevic, M., Buizert, C., Jenk, T. M., Sapart, C. J., Schaefer, H., Popp, T. J., and Blunier, T.: A combustion setup to precisely reference $\delta^{13}C$ and $\delta^{2}H$ isotope ratios of pure CH_4 to produce isotope reference gases of $\delta^{13}C$-CH_4 in synthetic air, Atmos. Meas. Tech., 5, 2227-2236, doi:10.5194/amt-5-2227-2012, 2012.

Sperlich, P., Buizert, C., Jenk, T. M., Sapart, C. J., Prokopiou, M., Röckmann, T., and Blunier, T.: An automated GC-C-GC-IRMS setup to measure palaeoatmospheric $\delta^{13}C$-CH_4, $\delta^{15}N$-N_2O and $\delta^{18}O$-N_2O in one ice core sample, Atmos. Meas. Tech., 6, 2027-2041, doi:10.5194/amt-6-2027-2013, 2013.

Sperlich, P., Schaefer, H., Mikaloff Fletcher, S. E., Guillevic, M., Lassey, K., Sapart, C. J., Röckmann, T., and Blunier T.: Carbon isotope ratios suggest no additional methane from boreal wetlands during the rapid Greenland Interstadial 21.2, Global Biogeochem. Cycles, 29, 1962–1976, doi:10.1002/2014GB005007, 2015.

Sperlich, P., Uitslag, N. A. M., Richter, J. M., Rothe, M., Geilmann, H., van der Veen, C., Röckmann, T., Blunier, T., and Brand, W. A.: Development and evaluation of a suite of isotope reference gases for methane in air, Atmos. Meas. Tech., 9, 3717–3737, doi:10.5194.amt-9-3717-2016, 2016.

Stevens, C. M. and Rust, F. E.: The Carbon Isotopic Composition of Atmospheric Methane, J. Geophys. Res.-Ocean. Atmos., 87, 4879–4882, doi:10.1029/JC087iC07p04879, 1982.

Sugawara, S., Nakazawa, T., Inoue, G., Machida, T., Mukai, H., Vinnichenko, N. K., and Khattatov, V. U.: Aircraft measurements of the stable carbon isotopic ratio of atmospheric methane over Siberia, Global Biogeochem. Cy., 10(2), 223–231, doi:10.1029/96GB00038, 1996.

Teama, D. G. M., A 30-Year Record of the Isotopic Composition of Atmospheric Methane, Dissertations and Theses. Paper 642, http://pdxscholar.library.pdx.edu/open_access_etds/642, doi:10.15760/etd.642, 2013.

Turner, A. J., C. Frankenberg, C., Wennberg, P. O., and Jacob, D. J.: Ambiguity in the causes for decadal trends in atmospheric methane and hydroxyl, Proc. Natl. Acad. Sci., 114, 21, 5367–5372, doi:10.1073/pnas.1616020114, 2017.

Tyler, S. C., Ajie, H. O., Gupta, M. L., Cicerone, R. J., Blake, D. R., and Dlugokencky, E. J.: Stable carbon isotopic composition of atmospheric methane: A comparison of surface level and free tropospheric air, J. Geophys. Res., 104, 13895–13910, doi:10.1029/1999JD900029, 1999.

Tyler, S. C., Rice, A. L., and Ajie, H. O.: Stable isotope ratios in atmospheric CH_4: Implications for seasonal sources and sinks, J. Geophys. Res., 112, D03303, doi:10.1029/2006JD007231, 2007.

Umezawa, T., Aoki, S., Nakazawa, T., and Morimoto, S.: A High-precision Measurement System for Carbon and Hydrogen Isotopic Ratios of Atmospheric Methane and Its Application to Air Samples Collected in the Western Pacific Region, J. Meteorol. So. Jpn, 87, 365–379, doi:10.2151/jmsj.87.365, 2009.

Umezawa, T., Machida, T., Ishijima, K., Matsueda, H., Sawa, Y., Patra, P. K., Aoki, S., and Nakazawa, T.: Carbon and hydrogen isotopic ratios of atmospheric methane in the upper troposphere over the Western Pacific, Atmos. Chem. Phys., 12, 8095-8113, doi:10.5194/acp-12-8095-2012, 2012a.

Umezawa, T., Machida, T., Aoki, S. and Nakazawa, T.: Contributions of natural and anthropogenic sources to atmospheric methane variations over western Siberia estimated from its carbon and hydrogen stable isotopes, Global Biogeochem. Cycles, 26, GB4009, doi:10.1029/2011GB004232, 2012b.

Umezawa, T., Goto, D., Aoki, S., Ishijima, K., Patra, P. K., Sugawara, S., Morimoto, S., Nakazawa, T.: Variations of tropospheric methane over Japan during 1988–2010, Tellus B, 66, 23837, doi:10.3402/tellusb.v66.23837, 2014.

Wendeberg, M., Richter, J. M., Rothe, M., and Brand, W. A.: Jena Reference Air Set (JRAS): a multi-
5 point scale anchor for isotope measurements of CO_2 in air, Atmos. Meas. Tech., 6, 817-822, doi:10.5194/amt-6-817-2013, 2013.

Verkouteren, R. M., Allison, C. E., Studley, S. A., and Leckrone, K. J.: Isotopic metrology of carbon dioxide. I. Interlaboratory comparison and empirical modeling of inlet equilibration time, inlet pressure, and ion source conductance, Rapid Commun. Mass Sp., 17, 771–776, doi:10.1002/rcm.905, 2003a.

10 Verkouteren, R. M., Assonov, S., Klinedinst, D. B., and Brand, W. A.: Isotopic metrology of carbon dioxide. II. Effects of ion source materials, conductance, emission, and accelerating voltage on dual-inlet cross contamination, Rapid Commun. Mass Sp., 17, 777–782, doi:10.1002/rcm.906, 2003b.

Werner R. A. and Brand, W. A.: Referencing strategies and techniques in stable isotope ratio analysis, Rapid Commun. Mass Sp., 15, 501–519, doi:10.1002/rcm.258, 2001.

15 White, J.W.C., B.H. Vaughn, and S.E. Michel (2016), University of Colorado, Institute of Arctic and Alpine Research (INSTAAR), Stable Isotopic Composition of Atmospheric Methane (^{2}H) from the NOAA ESRL Carbon Cycle Cooperative Global Air Sampling Network, 2005-2009, Version: 2016-04-26, Path: ftp://aftp.cmdl.noaa.gov/data/trace_gases/ch4h2/flask/.

World Meteorological Organization: 18th WMO/IAEA Meeting on carbon dioxide, other greenhouse
20 gases, and related measurement techniques (GGMT-2015), GAW report No. 229, 2016.

Table 1. List of laboratories that conduct measurements of δ^{13}C-CH$_4$ and δD-CH$_4$. For each laboratory, measurement systems and relevant information that could have contributed the inter-laboratory measurement offsets are summarized. Brackets in the RM column indicate the laboratory from which the original standard scale was propagated. See Figure 1 for overview of the past intercomparison exercises, Figure 2 for intercomparison summary and the list of participating institution/project acronyms in the text for the laboratory names.

No	Lab	System	IRMS	^{17}O correction[*]	Kr interference		Additional Correction	RM		Reference[‡]			δ^{13}C-CH$_4$ offset with respect to NIWA	δD-CH$_4$ offset with respect to IMAU	Data Availability[§]
					Significance	Measure[†]				Measurement	Intercomparison				
								δ^{13}C-CH$_4$	δD-CH$_4$		δ^{13}C-CH$_4$	δD-CH$_4$			
1	NIWA	DI	Nuclide (1988–1996) MAT 252 (1996–2013) MAT 253 (2013–)	C1/C2	N	—	N	NBS-19, IAEA-CO-9, LSVEC	Not measured	R1	R2, R3, R4, R5, R6, R7, R8, R9, R10, R11, R12, R13	Not measured	—	Not Measured	WDCGG & NIWA website (R1, R2, R14)
		CF	Isoprime	C3	Y	DI offset/PCS	Drift			R15, R16					On request to H. Schaefer (R17)
2	IMAU	CF	Delta plus XL	C2	Y	PCS	Non-linearity correction for small peaks	NBS-19 (MPIC)	VSMOW & SLAP (MPIC)	R18	R10, R12, R18, R19, R20, R21, R22, R23	R12, R18, R20, R21, R22, R23, R24	−0.04±0.07	—	Utrecht University website (R25, R26)
3	MPIC	DI & TDLAS	MAT 252	C2	N	—	N	NBS-19	VSMOW & SLAP	R27	R18, R19	R18, R24	−0.04±0.07	+0.3±1.1	On request to P. Bergamaschi (R28)
4	MPI-BGC	CF	Delta V Plus	C4	Y	PCS	Mole fraction dependent linearity correction	NBS-19 & LSVEC	VSMOW-2 & SLAP-2	R29	R21, R30	R21, R30	−0.07±0.12	−4.2±1.2	On request to H. Moossen (R21, R29)
5	UCI	DI	MAT 252	C2	N	—	N	NBS-19 & IAEA-CO-9	Oztech Gas	R7, R31	R7, R12, R15, R22, R32, R33	R22, R33	−0.01±0.09	−10.7±0.7	CDIAC (R31)
		CF	Delta Plus XL	C2	Y	DI offset/PCS	N			R7, R34					

6	TU	CF	Delta Plus XP	C3	Y	No	Daily correction with respect to a test gas; Constant offset for part of the dataset (R34, R35)	NBS-19	VSMOW & SLAP	R37	R23, R37	R23	+0.36±0.08	−13.1±0.6	WDCGG (R35) & On request to T. Umezawa (R36, R38)
7	NIPR	CF	MAT 252	C3	N	—	N	NBS-19 (TU)	Not measured	R8	R8, R23, R37	Not measured	+0.33±0.04	Not measured	TU website (R8, R39)
8	UW	DI	MAT 251	Information not available	N	—	Correction of N$_2$O produced during combustion & Drift correction	NBS-19	VSMOW & SLAP	R3	R2, R3, R4, R32	No comparison available	+0.02±0.14	No comparison	CDIAC (R3)
9	UHEI	DI	MAT 252	C2 with coefficients a=0.5 & K=0.008335	N	—	Drift correction of extraction and daily correction of IRMS	RM 8562, RM 8563 & RM 8564	VSMOW & SLAP	R5	R4, R5, R6, R19, R30	R30	−0.17±0.03	−3.8±1.3	UHEI website (R4)
10	INSTAAR	CF	Optima/Isoprime	C3	Y	PCS	Drift correction	NBS-19 & IAEA-CO-9 (UCI)	Not Anchored	R15	R4, R7, R9, R11, R12, R13, R15, R19, R41	R24	+0.13±0.02	−13.2±1.3	WDCGG & NOAA/ESRL/GMD website (R15)
11	RHUL	DI / CF	Prism / Isoprime	C3	N	—	Daily offset with respect to working air standard	NBS-19 & IAEA-CO-9	Not measured	R42 / R43	R9, R11, R13	Not measured	+0.12±0.03	Not measured	CEDA & On request to E. Nisbet (R11)
12	PDX	CF	Delta V	C2	Y	DI offset/PCS	N	NBS-19 & IAEA-CO-9 (UCI)	Oztech Gas (UCI)	R33, R34	R32, R33	R32, R33	+0.08±0.09	−10.7±1.5	PDX website (R32)
13	PSU	CF	MAT 252	C2	Y	Raw ion current correction/ DI offset/PCS	Daily offset with respect to primary air standard	RM 8563 & RM 8564	Oztech Gas	R20, R44	R10, R12, R19, R20	R12, R20, R24	+0.03±0.16	−12.1±1.5	NSIDC & On request to T. Sowers
14	UB	CF	Isoprime	C2	Y	PCS	Drift correction	NBS-19 & IAEA-CO-9 (UCI via	VSMOW & SLAP (UHEI)	R10, R24, R41,	R10, R12, R20,	R12, R20, R24,	−0.18±0.09	0.0±1.6	PANGAEA (R46, R47)

								INSTAAR)		R45	R41	R45			
15	AWI	CF	Isoprime	C3	Y	No	Drift correction	RM 8562, RM 8563 and RM 8564 (UHEI)	Not measured	R6	R6, R10, R19, R20	Not measured	−0.09±0.06	Not measured	PANGAEA (R19)
16	CIC	DI (δ^{13}C-CH$_4$) TC/EA-IRMS & Picarro (δD-CH$_4$)	Delta V Plus, Delta V Advantage and Picarro	C2	N	—	—	RM 8563	VSMOW-2 & SLAP-2	R48	R21, R48	R21, R48	−0.03±0.11	−2.1±2.1	All data in papers (R16, R21, R48)
		CF	Delta V Plus	C2	Y	PCS	Daily offset with respect to working gas standard; CH$_4$ amount correction		Not measured	R16	R16				

[*]C1: Allison et al. (1995), C2: Santrock et al. (1985), C3: Craig (1957), C4: Assonov and Brenninkmeijer (2003)

[†]Raw ion current correction: The Kr effect was corrected by subtracting the Kr-caused anomalies in the raw ion current data; DI offset: The Kr effect was corrected by an offset relative to a DI-IRMS measurement; PCS: Kr was separated by a post combustion separation column or cryogenically. See section 2.5.

[‡]R1: Lowe et al. (1991), R2: Lowe et al. (1994), R3: Quay et al. (1999), R4: Levin et al. (2012), R5: Poß (2003), R6: Behrens et al. (2008), R7: Tyler et al. (2007), R8: Morimoto et al. (2006), R9: Nisbet (2005), R10: Schmitt et al. (2013), R11: Nisbet et al. (2016), R12: This study (Section 4.4), R13: This study (Section 4.6), R14: Bergamaschi et al. (2001), R15: Miller et al. (2002), R16: Sperlich et al. (2013), R17: Ferretti et al. (2005), R18: Brass and Röckmann (2010), R19: Möller et al. (2013), R20: Sapart et al. (2011), R21: Sperlich et al. (2016), R22: This study (Section 4.1), R23: This study (Section 4.2), R24: Bock et al. (2010a), R25: Röckmann et al. (2010), R26: Röckmann et al. (2016), R27: Bergamaschi et al. (1994), R28: Bergamaschi et al. (2000); R29: Brand et al. (2016), R30: This study (Section 4.3), R31: Tyler et al. (1999), R32: Rice et al. (2016), R33: Teama (2013), R34: Rice et al. (2001), R35: Umezawa et al. (2012a), R36: Umezawa et al. (2012b), R37: Umezawa et al. (2009), R38: Umezawa et al. (2011), R39: Morimoto et al. (2017), R40: This study (Section 4.3), R41: Schmitt et al. (2014), R42: Lowry et al. (2001), R43: Fisher et al. (2006), R44: Sowers et al. (2005), R45: Bock et al. (2014); R46: Bock et al. (2010b), R47: Bock et al. (2017), R48: Sperlich et al. (2012)

[§]WDCGG (World Data Centre for Greenhouse Gases): http://ds.data.jma.go.jp/gmd/wdcgg/wdcgg.html
NIWA website: www.niwa.co.nz
Utrecht University website: http://www.projects.science.uu.nl/atmosphereclimate/Data.php
TU website (http://caos.sakura.ne.jp/tgr/data/en)
CDIAC (Carbon Dioxide Information Analysis Center): http://cdiac.ess-dive.lbl.gov/epubs/db/db1022/db1022.html (UCI), http://cdiac.ess-dive.lbl.gov/ndps/quay.html (UW)
UHEI website: www.iup.uni-heidelberg.de/institut/forschung/groups/kk/Data_html
NOAA/ESRL/GMD website: https://www.esrl.noaa.gov/gmd/dv/data/
PDX website: http://web.pdx.edu/~arice/atm_CH4.html
PANGAEA: https://doi.org/10.1594/PANGAEA.873918
CEDA (Centre for Environmental Data Analysis): http://www.ceda.ac.uk
H. Schaefer: h.schaefer@niwa.co.nz
P. Bergamaschi: peter.bergamaschi@ec.europa.eu
H. Moossen: heiko.moossen@bgc-jena.mpg.de
T. Umezawa: umezawa.taku@nies.go.jp
E. G. Nisbet: e.nisbet@rhul.ac.uk
T. Sowers: tas11@psu.edu

Table 2. Result of intercomparison of $\delta^{13}C$-CH_4 and δD-CH_4 measurements between UCI and IMAU.

Sample ID	CH_4 (ppb)	$\delta^{13}C$-CH_4 (‰) UCI	IMAU	Difference from IMAU	δD-CH_4 (‰) UCI	IMAU	Difference from IMAU
WAS-24-2	1784.7[*]	−46.96±0.07 (N=3)	−47.33±0.05 (N=3)	+0.37	−91.6±0.5 (N=2)	−78.9±0.1 (N=4)	−12.7
WAS-24-5	1825.8[*]	−47.16 (N=1)	−47.53±0.02 (N=6)	+0.37	−93.8 (N=1)	−83.1±0.2 (N=4)	−10.7
WAS-24-6	1827.5[*]	−47.08±0.01 (N=2)	−47.55±0.04 (N=6)	+0.47	−92.1±0.8 (N=2)	−83.6±0.1 (N=4)	−8.5
WAS-24-9	1799.8[*]	−47.05 (N=1)	−47.38±0.02 (N=6)	+0.33	−92.3±1.8 (N=3)	−79.8±0.8 (N=4)	−12.4
WAS-24-10	1789.8[*]	−47.07 (N=1)	−47.42±0.02 (N=6)	+0.35	−89.3 (N=1)	−79.7±0.8 (N=4))	−9.6
WAS-24-11	1780.8[*]	−46.77 (N=1)	−47.37±0.03 (N=6)	+0.60	−89.0±0.9 (N=2)	−78.7±0.7 (N=4)	−10.3
Average				+0.42±0.04			−10.7±0.7

[*]NOAA-2004 CH_4 scale (Dlugokencky et al., 2005)

Table 3. Result of intercomparison of $\delta^{13}C$-CH_4 and δD-CH_4 measurements between TU/NIPR and IMAU.

Sample ID	CH_4 (ppb)[*]	$\delta^{13}C$-CH_4 (‰) TU	NIPR	IMAU	Difference from IMAU	δD-CH_4 (‰) TU	IMAU	Difference from IMAU
MD1	1901.1	−47.04±0.02 (*N*=16)	−47.11±0.02 (*N*=5)	−47.40±0.04 (*N*=9)	+0.36 (TU) +0.28 (NIPR)	−97.2±0.6 (*N*=10)	−85.0±0.1 (*N*=8)	−12.2
MD2	2116.6	−46.81±0.02 (*N*=16)	−46.92±0.03 (*N*=6)	−47.26±0.03 (*N*=9)	+0.45 (TU) +0.34 (NIPR)	−118.5±0.6 (*N*=10)	−104.5±0.3 (*N*=8)	−14.0
MD3	899.1	−41.14±0.04 (*N*=16)	−41.05±0.02 (*N*=5)	−41.81±0.03 (*N*=8)	+0.67 (TU) +0.76 (NIPR)	−190.7±0.6 (*N*=10)	−175.8±0.6 (*N*=8)	−14.9
MD4	1700.5	−42.47±0.03 (*N*=16)	−42.43±0.04 (*N*=5)	−42.98±0.02 (*N*=8)	+0.52 (TU) +0.56 (NIPR)	−195.2±0.6 (*N*=10)	−180.6±0.2 (*N*=8)	−14.6
Average (ambient air)					+0.40±0.04 (TU) +0.31±0.03 (NIPR)			−13.1±0.6
Average (all)					+0.50±0.07 (TU) +0.48±0.11 (NIPR)			−13.9±0.9

[*]Tohoku University CH_4 scale (Aoki et al., 1992; Umezawa et al., 2014)

Table 4. Result of intercomparison of δ^{13}C-CH$_4$ and δD-CH$_4$ measurements between UHEI and MPI-BGC.

Sample ID (Collection Date)	Preparation Date UHEI	Analysis Date MPI-BGC	δ^{13}C-CH$_4$ (‰) UHEI	MPI-BGC[*]	UHEI −MPI-BGC	δD-CH$_4$ (‰) UHEI	MPI-BGC[*]	UHEI −MPI-BGC
GvN 88/20 (24 Jul. 1988)	17 Dec. 2003	9 Jul. 2013	−47.54±0.02 (N=1)	−47.66 (0.07, N=2)	+0.13	−83.3±2.2 (N=1)	−82.1 (0.8, N=2)	−1.2
GvN 92/12 (11 May. 1992)	11 Dec. 2008	17 Jun. 2013	−47.43±0.02 (N=1)	−47.40 (0.04, N=2)	−0.03	−79.1±1.6 (N=1)	−81.2 (0.9, N=2)	+2.1
GvN 96/03 (13 Feb. 1996)	11 Nov. 2003	17 Jun. 2013	−47.27±0.02 (N=1)	−47.18 (0.26, N=2)	−0.08	−73.9±1.4 (N=2)	−74.6 (0.9, N=2)	+0.8
GvN 99/14 (29 Dec. 1999)	3 Apr. 2003	9 Jul. 2013	−47.30±0.02 (N=1)	−47.23 (0.16, N=2)	−0.07	−75.2±1.3 (N=2)	−74.6 (1.3, N=2)	−0.5
GvN 06/14 (23 Sep. 2006)	7 May. 2003	9 Jul. 2013	n.a.	−47.19 (0.09, N=2)	n.a.	−72.3±1.6 (N=1)	−73.1 (0.0, N=2)	+0.8
GvN 08/03 (6 Mar. 2008)	28 Jul. 2010	17 Jun. 2013	−47.18±0.05 (N=1)	−47.35 (0.05, N=2)	+0.17	n.a.	−67.4 (2.9, N=2)	n.a.
Average					+0.02±0.05			+0.4±0.6

[*]Difference of duplicate flask measurements is shown in parenthesis.

Table 5. Results from the Ice Core Intercomparison Round Robin conducted during 2007–2016.

Laboratory	CA 03560 (1830.6 ppb)		CA 71560 (904.0 ppb)		CA 01179 (372.2 ppb)		Kr corr.	Analysis Date δ^{13}C-CH$_4$	Analysis Date δD-CH$_4$
	δ^{13}C-CH$_4$ (‰)	δD-CH$_4$ (‰)	δ^{13}C-CH$_4$ (‰)	δD-CH$_4$ (‰)	δ^{13}C-CH$_4$ (‰)	δD-CH$_4$ (‰)			
PSU	−47.20±0.16	−93.2±0.9	−47.41±0.10	−95.5±2.3	−47.52±0.06	−106.3±2.4	Raw ion current correction[a]	Jul. 2007	Jul. 2007
	−46.96±0.16		−47.20±0.10		−47.41±0.12		DI offset[b]	Jul. 2007	
	−47.10±0.05		−47.09±0.06		−46.83±0.12		PCS[c]	May 2016	
UCI (DI-IRMS)	−47.09±0.12		−47.40±0.08		−47.23±0.06		—	Dec. 2007[*]	
INSTAAR	−47.08±0.05		−47.20±0.06		−46.78±0.06		PCS[c]	Dec. 2008	
NIWA (DI-IRMS)	−47.23±0.02		−47.44±0.02		−47.43±0.02		—	Jun. 2009	
NIWA (GC-IRMS)	−47.44±0.21		−48.34±0.28		−47.62±0.11		DI offset[b]	Jun. 2009	
UB	−47.41±0.09	−80.4±2.2	−47.37±0.07	−81.0±2.0	−47.31±0.11	−86.2±3.3	No[d]	Jan. 2011	Dec. 2010–Jan. 2011
IMAU	−47.27±0.07	−79.6±1.2	−47.52±0.11	−83.6±3.8	−47.20±0.20	−78.8±12.4	PCS[c]	May & Aug. 2012	May 2010

[a]Raw ion current correction: The Kr effect was corrected by subtracting the Kr-caused anomalies in the raw ion current data (section 5.4 of Schmitt et al., 2013); [b]DI offset.: The Kr effect was corrected by an offset relative to a DI-IRMS measurement; [c]PCS: Kr was separated by a post combustion separation column (section 5.2 of Schmitt et al. 2013); [d]No: Measurements are affected by the Kr interference (old

5   system without PCS) and raw ion current correction was not possible.

[*]Estimated because no exact record on the analysis date at UCI is unfortunately available.

Table 6. Results of δ^{13}C-CH$_4$ intercomparison between INSTAAR and MPI-BGC.

| Sample ID | CH$_4$ (ppb)[*] | δ^{13}C-CH$_4$ (‰) | | INSTAAR−MPI-BGC |
		INSTAAR	MPI-BGC	
HUEY-001	1905.5	−47.37±0.01	−47.67±0.01	+0.29
		(*N*=22)	(*N*=24)	
DEWY-001	1879.9	−47.38±0.01	−47.67±0.01	+0.28
		(*N*=26)	(*N*=22)	
LOUI-001	1496.0	−47.26±0.01	−47.55±0.02	+0.29
		(*N*=17)	(*N*=22)	
CART-001	1848.1	−42.98±0.01	−43.30±0.03	+0.32
		(*N*=21)	(*N*=7)	
STAN-001	1696.4	−56.60±0.01	−57.20±0.05	+0.60
		(*N*=7)	(*N*=8)	
KENN-001	1847.6	−47.65±0.01	−47.94±0.05	+0.28
		(*N*=26)	(*N*=7)	
KYLE-001	1847.6	−47.27±0.01	−47.51±0.07	+0.24
		(*N*=29)	(*N*=6)	

[*]NOAA-2004 CH$_4$ scale (Dlugokencky et al., 2005)
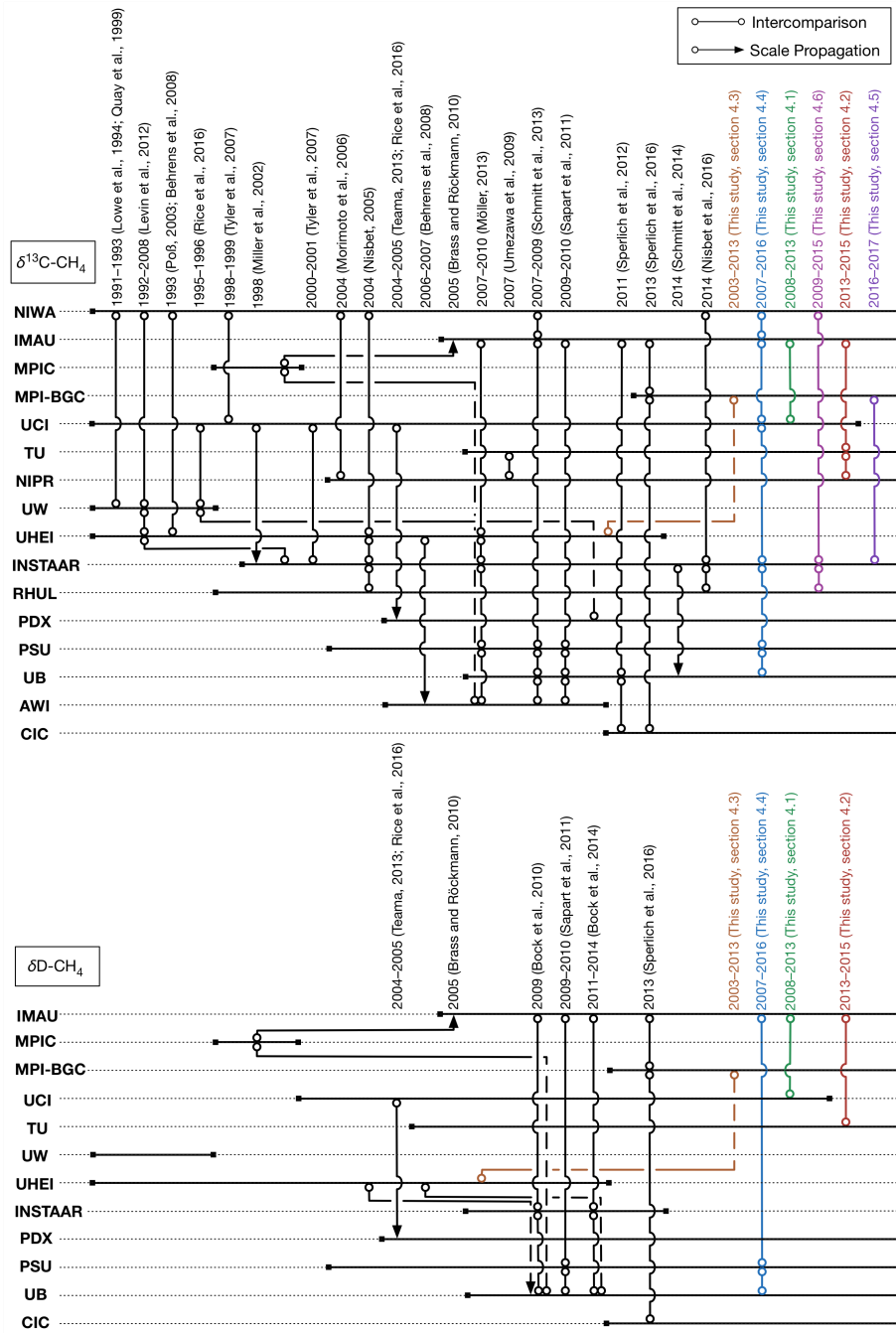
Figure 1. A schematic overview of the previous and present intercomparisons between laboratories for δ^{13}C-CH$_4$ (top) and δD-CH$_4$ (bottom). Intercomparisons are marked by lines with open circles at both ends, and scale propagations are by lines with an arrow at one end.
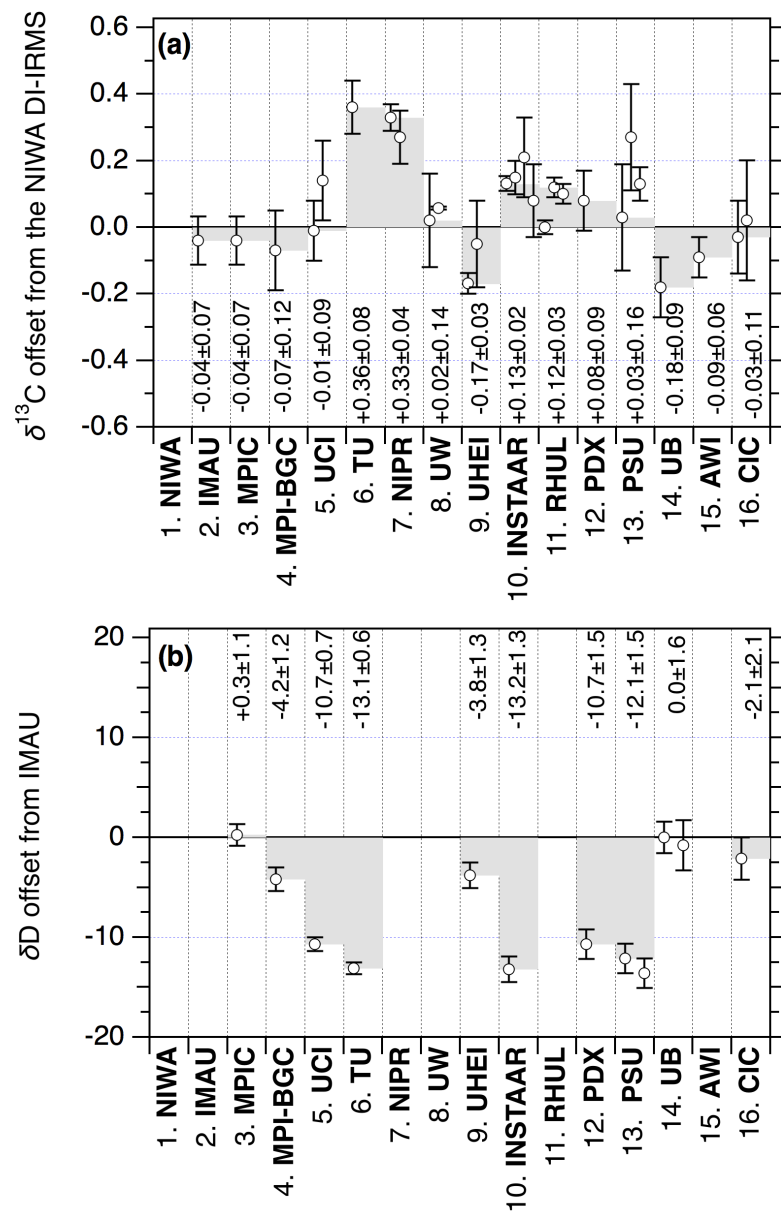
Figure 2. (a) δ^{13}C-CH$_4$ offsets of the different laboratories with respect to the NIWA DI-IRMS measurement with gray shades for ease of viewing. (b) δD-CH$_4$ offsets of the different laboratories with respect to the IMAU GC-IRMS measurement. See Table 1 and text for corresponding subsections in sections 3 and 5. Numbers shown in each laboratory column are the plausible measurement offsets estimated in this study. Note that this result represents intercomparisons for the modern atmospheric CH$_4$.